Pirathayini Srikantha and Deepa Kundur

Intelligent Signal Processing and Coordination for the Adaptive Smart Grid

An overview of data-driven grid management

Digital Object Identifier 10.1109/MSP.2018.2877001
Date of publication: 26 April 2019

In today's era of the Internet of Things (IoT), the amalgamation of information and communication technologies with actuating devices has reached all corners of the modern world. In the context of critical infrastructures, such as the power grid, this cyberphysical transformation has permeated all system levels as evident in devices ranging from crucial operational components (e.g., generators) and advanced sensors [e.g., phasor measurement units (PMUs) and programmable controllers], to consumer-centric devices [smart meters, electric vehicles (EVs), and smart appliances]. These extended cyberphysical functionalities have opened up signal processing opportunities that can be harnessed to empower actuating devices to adaptively and synergistically acquire data, conduct analytics, and respond to system and environmental changes for better power-grid operations. In this article, we demonstrate how a hierarchical signal processing and actuation framework can enable the tractable all-encompassing coordination of thousands of actuating power entities to maintain efficient operations while accounting for physical infrastructure limits.

Adaptive monitoring and control

Revolutionary changes in clean energy policies along with advances in technologies related to power-consumption and power-generation technologies are triggering a major paradigm shift in the electricity sector [1]. This shift is blurring conventional boundaries in the vertically integrated power grid. With deregulation in electricity markets and the introduction of sustainability incentives, independent power plants (IPPs), consisting of highly fluctuating renewable energy sources, and alternative loads, such as EVs, have become more common. In increasing numbers, power consumers are also becoming sellers as they deploy microgeneration systems to supplement local electricity needs. Amid this rapidly evolving landscape of electricity supply and demand, upgrades to the underlying power infrastructure consisting of transmission/distribution lines, transformers, and protection devices are falling behind [2]. Meanwhile, cyberenabled sensors and actuators are being widely deployed across all levels of the power grid. These resources can be leveraged to enable adaptive monitoring and control to overcome the arising challenges by capitalizing on recent advances in data analytics and intelligent signal processing techniques.

The modern grid must contend with growing congestion, inefficiency, and system vulnerabilities that can lead to costly equipment damage and, eventually, cascading failures.

Ongoing changes in the traditional grid

The traditional grid is designed to accommodate a centralized power infrastructure in which power flows from bulk synchronous generation systems to consumers, as illustrated in Figure 1. The output from these bulk-power plants is predictable, as the prime movers are fueled by nuclear, gas, coal, or hydroelectric sources directly maintained by system operators [3]. High-voltage transmission networks (TNs) facilitate the transportation of generated power across geographically dispersed regions. In recent years, TNs have come to include solar and wind farms and other IPPs as alternatives to bulk-generation plants based on fossil fuels and associated with large carbon footprints. Due to the intermittent nature of solar and wind energy, TN lines are experiencing unpredictable periods of congestion that cause the system to function perilously close to stable limits.

Distribution networks (DNs) operate at low voltages and tap onto the TN to deliver power to local consumers. With the significant proliferation of distributed generation (DG) systems in the DN, sudden surges in generation can lead to voltage spikes, which result in overvoltage conditions. Similarly, the deployment of large power-consuming equipment, such as EVs in the DNs, can result in voltage drops that can lead to undervoltage conditions. These voltage violations can trigger passive protection elements, such as fuses and circuit breakers, which can result in outages requiring hours to reinstate [4].

Hence, the modern grid must contend with growing congestion, inefficiency, and system vulnerabilities that can lead to costly equipment damage and, eventually, cascading failures. Upgrading the grid infrastructure to better accommodate these changes is extremely costly [1]. However, opportunities lie in the effective use of vast volumes of grid-monitoring data generated every second by measuring devices and in offloading decision making to actuating power components by way of intelligent signal processing. Designing signals that capture the general trends in the power grid and efficiently processing these to adaptively compute local actuation decisions enable more efficient and cost-effective grid operations.

Opportunities in the cyberphysical power grid

Widespread connectivity permeating modern society has triggered the IoT era [5]. Devices ranging from wearables

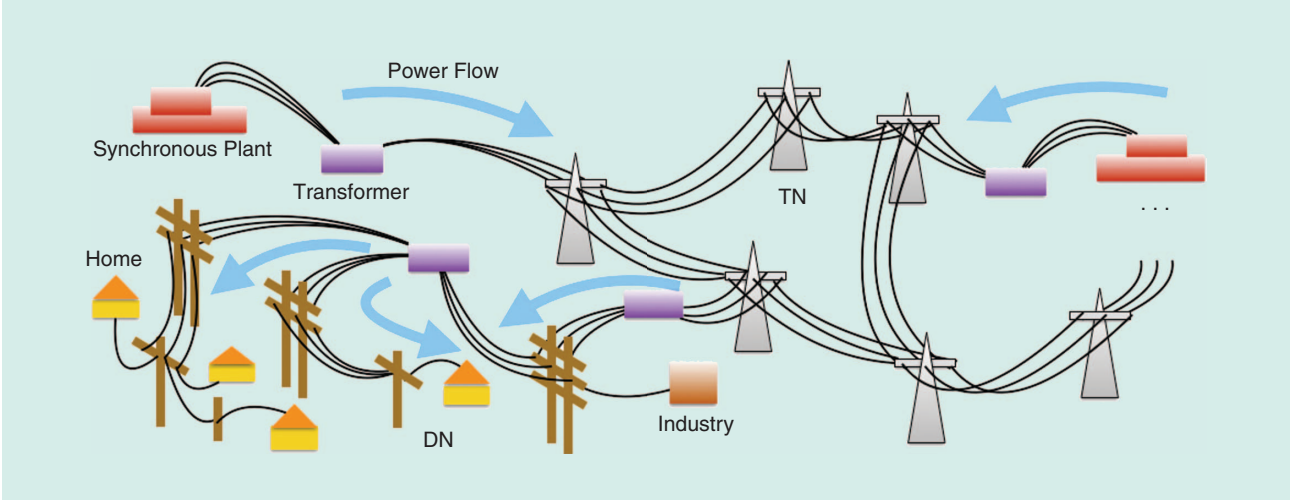

FIGURE 1. A traditional grid.

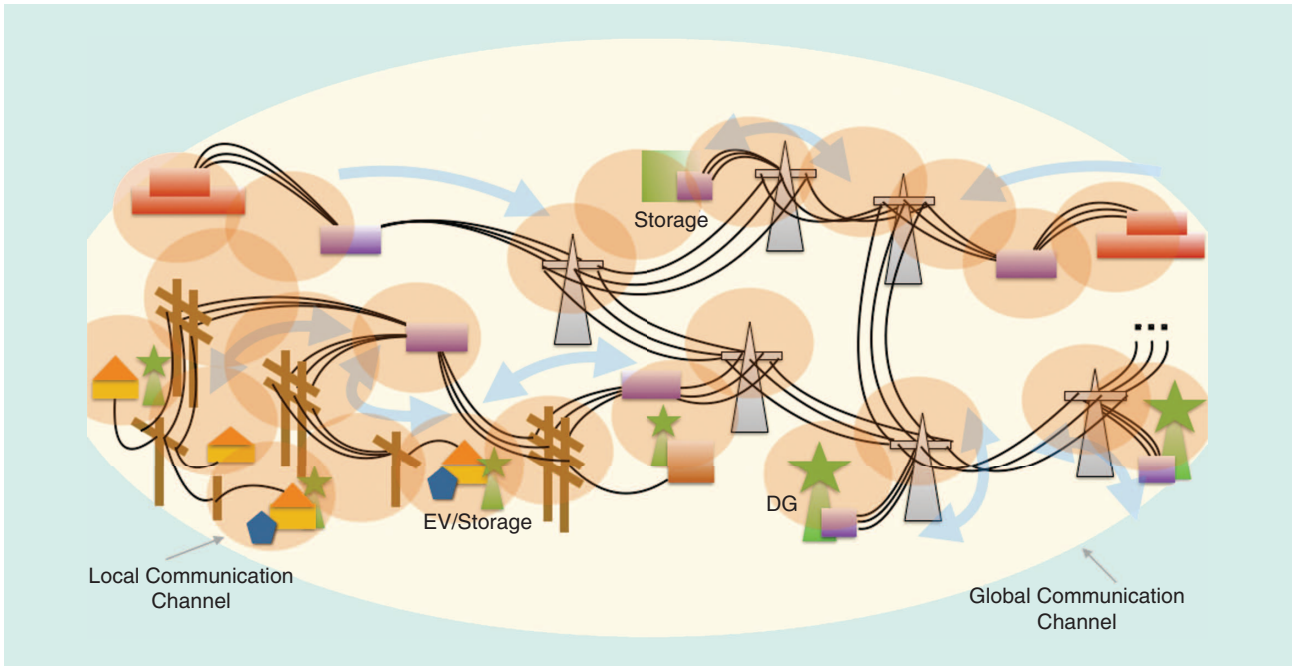

FIGURE 2. The cyberphysical smart grid.

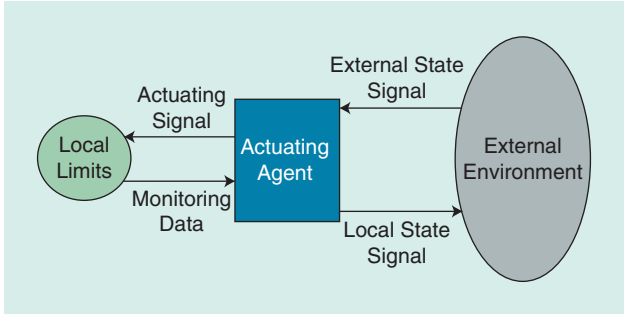

FIGURE 3. Adaptive actuation.

to critical infrastructure elements can communicate, perform computations locally, and intelligently actuate. As illustrated in Figure 2, the modern grid is just one of many parts of our world where cyberphysical amalgamation—the development of interacting networks of computational and physical components—is taking place. The vast majority of consumer appliances and grid management entities, such as circuit breakers, relays, transformers, and inverters, are smart. That is, they are capable of decision making facilitated by signal processing. In addition to these actuating devices, many monitoring devices, such as smart meters and PMUs, are recording the states of the grid in a highly granular manner, thus providing opportunities for advanced data analytics. These monitoring and control systems currently in place constitute the smart grid [1]. The information-centric cyberenabled power grid elevates situational awareness and enables intelligent cyberphysical signal processing-enabled responses by active nodes to adaptively and effectively react to system changes.

Hierarchical coordination in the smart grid

The cyberphysical power grid is a monolithic entity made up of millions of active nodes. Coordinating these devices while accounting for underlying physical grid characteristics is an ongoing challenge for researchers due to the immense number of controllable elements present in the system and the inclusion of nonlinear physical constraints embodying power balance and bus/line limits. Moreover, the highly varying nature of active nodes, such as the renewables, introduces significant actuation signal uncertainty due to significant error margins present in the associated long-term generation-forecast models [6]. Thus, applying the traditional vertically integrated grid-operation model, whereby active elements and signal processing are centrally coordinated, is not practical.

The unified hierarchical framework introduced in this article presents signal processing mechanisms by which concentrated computational efforts are offloaded to every actuating element in the system so that they can adaptively react to improve global power-system conditions. For this, key concepts involving decoupling, abstraction, decomposition, and parallel processing are leveraged. Figure 3 illustrates the fundamental principle used in the design of local decision making by every active node.

Information about the global state of the system with respect to highest efficiency and balance in physical constraints is communicated to each cyberenabled node via signals designed by processing grid-measurement data. These signals capture summary information regarding the state of the global system. In this article, we distinguish data and signals in the following manner. Raw state measurements generated by monitoring devices (e.g., smart

meters, PMUs) are referred to as *data*. Signals, meanwhile, contain insights obtained by strategically combining and processing these monitoring data. The nodes, upon receiving these signals, react to improve the external system state while accounting for local physical constraints. These summary signals can be exchanged among active nodes or broadcast to many nodes via dedicated coordinating entities. The frequency of signal exchange depends on the control horizon and tier in which the coordination is taking place.

For tractable analysis, the grid-coordination problem is decomposed into simpler signal processing subproblems based on the control horizon, grid topology, and underlying physical network constraints forming tiers within the proposed hierarchical framework. As illustrated in Figure 4, managing entities representing tiers exchange signals to coordinate the activities of the tiers. As these summary signals convey general trends but do not contain specific information about individual system entities, abstraction is introduced. This allows for the plug-and-play integration of system components because existing nodes need not be aware of the specifics associated with these changes to design local actuation signals. Thus, the hierarchical framework introduces a flexible mechanism to accommodate the changing landscape of power demand and supply by leveraging the cyberphysical signal processing possible in the modern grid.

The information-centric cyberenabled power grid elevates situational awareness and enables intelligent cyberphysical signal processing-enabled responses by active nodes to adaptively and effectively react to system changes.

This article differs from our recent work in [7], which presents a hierarchical framework for the TN and DN where coordination is exacted via two specific methods tailored separately for these individual systems. In this article, we present a generalized hierarchical framework with built-in flexibility in the way coordination is executed within each tier, which represents a particular system being coordinated. Furthermore, we provide a comprehensive overview of power-flow equations (including convex relaxations and $dq0$ transformations) in the context of a wide variety of settings (such as microgrids and system protection) along with many practical cases. We also present a broad overview of coordination paradigms based on centralized, distributed, and decentralized techniques that can be flexibly applied to any tier of the hierarchical framework based on the power entities being coordinated, the system model considered, and the control horizon in place.

Hierarchical coordination can be applied to various components of the power grid. For instance, the primary, secondary, and tertiary control in place in today's electric grid is a hierarchical coordination mechanism. Primary control deals with real-time transients and, therefore, is typically decentralized. Secondary coordination involves the centralized computation of optimal generation setpoints. Tertiary control mechanisms, such as automatic generation controls (AGCs), are decentralized as local measurements, and computations are used for frequency control over wide areas. Thus, various coordination strategies are employed for the hierarchical management of systems ranging from bulk-power grids to microgrids [9]. This hierarchical paradigm can be used to coordinate active nodes at an even more granular manner across a broad range of control horizons while engaging not only generation entities but also active consumers, protective devices, and other actuating entities. Each tier can employ different types of

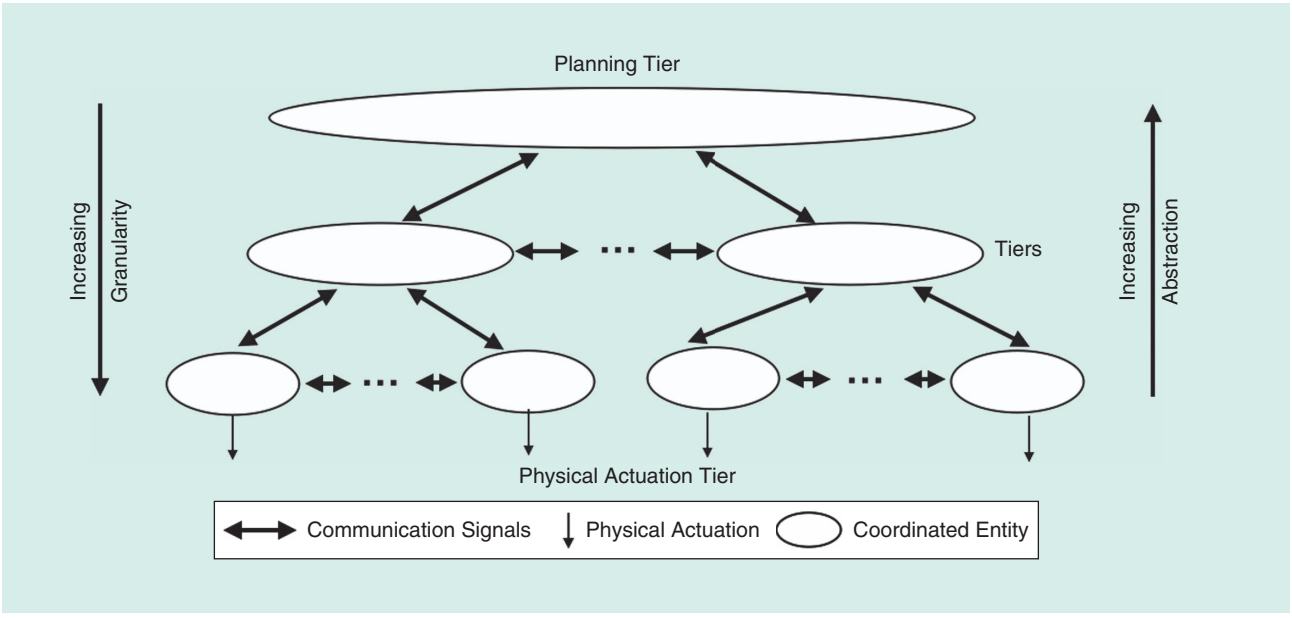

FIGURE 4. The hierarchical framework.

coordination strategies (such as centralized, decentralized, or distributed paradigms), which are associated with tradeoffs, including control horizon, error margin in forecast models, and presence of a centralized coordinating entity, to mention a few. The intratier and intertier interactions are governed by signals designed using underlying system constraints of the corresponding tiers and optimization goals.

Contributions of this article

The effective design of various tiers, signal processing topologies within these tiers, and adaptive decision making entails the following key considerations:

1) structure of the physical infrastructure (i.e., radial DN versus mesh TN, low voltage versus high voltage, and so on)
2) operational norms and ownership [e.g., deregulation, electric power utility (EPU), and so on]
3) signal processing and actuation horizon (e.g., fast response for highly fluctuating entities and slower response for planning purposes)
4) practical alterations of grid model for scalable and effective design of signals (i.e., simplification of highly nonlinear grid constraints so that these capture important attributes of power balance while enabling tractable analysis)
5) convergence of adaptive decision making (e.g., diversions that can lead to system damage)
6) computational and communication overhead associated with designing and exchanging signals.

The proposed hierarchical framework will capitalize on signal processing techniques to support the plug-and-play integration of diverse power entities (e.g., renewables, flexible consumers, smart loads, and so on) across the grid; actuating nodes will be equipped with the ability to make preventative decisions that circumvent impending grid issues identified by iterative signal and information exchange; system resilience will be further strengthened by increasing stability margins via adaptive decision making facilitated by effective signal processing; and efficiency will be embedded into every actuation decision made by intelligent nodes via adaptive construction of monitoring and actuation signals. This article presents a detailed exposition of various design aspects of the proposed hierarchical grid-management framework using mathematical tools and techniques, such as convex optimization, multiagent systems, machine learning, game theory, and social learning. We include a detailed literature survey and practical simulations along with theoretical studies to validate the effectiveness of the proposed framework.

Tractable physical grid modeling

In the proposed framework, actuating nodes use signals to infer general trends in the system as well as local operating conditions. To design signals that capture the grid state with respect to highest efficiency and feasible grid operating conditions, the incorporation of realistic physical power-grid models is imperative. As such, in this section, essential electrical laws and limits governing power flow in the grid are first presented. Then, challenges incurred in directly incorporating these into the optimal grid coordination problem are highlighted. Finally, methods that can be leveraged to relax these relations into tractable forms while retaining defining physical attributes are presented in the context of the TNs, DNs, microgrids, and power consumers. These tractable formulations can be decomposed into simpler subproblems that can then be used to glean pertinent information from monitoring data to design succinct signals reflecting general trends in the system. These signals will then be used by actuating nodes to make adaptive decisions for iteratively achieving reliable and efficient grid operations.

Power flow and limits

In today's grid, the prevalent mode of operation is ac, in which voltages and currents vary in a sinusoidal manner. When no transience is present, the system operates under what is known as *steady-state* conditions, and this is the grid mode used by operators for planning purposes. The steady-state grid model is typically composed of power-balance equations and equipment limits. Power-balance equations dictate, for example, how power flows through lines from generation sources to consumers. Operational limits, in contrast, indicate the thresholds set for the safe operation of power equipment.

Power balance is essentially determined by applying Kirchhoff's voltage and current laws pertaining to steady-state ac systems. The power system is composed of buses $\mathcal{B}$ to which consumers and/or generators connect. There are four important variables associated with each bus $i \in \mathcal{B}$, and these are bus-voltage magnitude $|V_i|$, bus angle θ_i, net real-power p_i injection, and net reactive-power q_i injection. This article uses capital letters to represent complex variables. Complex voltage V_i and apparent power S_i can be expressed in rectangular form [9]

$$V_i = |V_i|\cos(\theta_i) + \mathbf{j}|V_i|\sin(\theta_i), \tag{1}$$

$$S_i = p_i + \mathbf{j}q_i, \tag{2}$$

where $\mathbf{j} = \sqrt{-1}$. Buses are connected to one another by power lines. Properties of line $i-j$ connecting buses i and j are encapsulated by the complex-valued line-admittance parameter

$$Y_{ij} = g_{ij} + \mathbf{j}b_{ij}, \tag{3}$$

where g_{ij} and b_{ij} are the conductance and susceptance constants. Complex power flow S_{ij} from bus i to j is a function of the bus voltages V_i, V_j and the line admittance Y_{ij}

$$S_{ij} = V_i(V_i - V_j)^* Y_{ij}^*. \tag{4}$$

For power balance to hold, the net complex power injected by bus i must be equal to the power flowing from that bus to neighboring buses j as

$$S_i = \sum_{j\in\mathcal{N}_i} S_{ij} = \sum_{j\in\mathcal{N}_i} V_i(V_i - V_j)^* Y_{ij}^*, \tag{5}$$

where $\mathcal{N}_i$ is a set representing buses that are directly connected to bus i via a single power line (i.e., neighbors). Equation (5) is a complex quadratic relation that can be equivalently expressed in terms of real values as

$$\begin{aligned} p_i &= \sum_{j\in\mathcal{N}_i}\Big(|V_i|^2 g_{i,j} - |V_i||V_j|g_{ij}\cos(\theta_i-\theta_j) \\ &\quad - |V_i||V_j|b_{ij}\sin(\theta_i-\theta_j)\Big) \\ q_i &= \sum_{j\in\mathcal{N}_i}\Big(|V_i|^2 b_{i,j} + |V_i||V_j|b_{ij}\cos(\theta_i-\theta_j) \\ &\quad - |V_i||V_j|g_{ij}\sin(\theta_i-\theta_j)\Big). \end{aligned} \tag{6}$$

It is evident that these power-balance equations are highly nonlinear.

Each bus can be connected to a set of generators and/or consumers. The net real- and reactive-power injection in bus i is the cumulative contribution of these demand and supply units

$$p_i = p_i^g - p_i^d, q_i = q_i^g - q_i^d, \tag{7}$$

where p_i^g and q_i^g represent total real- and reactive-power generation in bus i and p_i^d and q_i^d represent total real- and reactive-power demand in bus i. Power generation and demand are subject to the upper and lower limits

$$p_{-i}^g \le p_i^g \le \bar{p_i}^g, q_{-i}^g \le q_i^g \le \bar{q_i}^g. \tag{8}$$

Flexible power consumers residing at bus i who have adjustable loads enable power demands to vary within the thresholds

$$p_{-i}^d \le p_i^d \le \bar{p_i}^d, q_{-i}^d \le q_i^d \le \bar{q_i}^d. \tag{9}$$

Bus-voltage limits are also important considerations as these govern voltage stability

$$v_{-i} \le |V_i| \le \bar{v}_i. \tag{10}$$

Voltage magnitudes are typically maintained around $\pm 10\%$ of the nominal value 1 per unit (p.u.) to prevent equipment damage. Apparent power limit reflects the maximum square magnitude of complex power flow $|\bar{S}_{ij}|^2$ permissible through a power line, and this is a constant parameter dictated by the characteristics of the associated conductor used for the line

$$p_i^2 + q_i^2 \le |\bar{S}_{ij}|^2. \tag{11}$$

Every bus and line in the power grid is subject to constraints listed in (6)–(11). The state estimation of signals generated by measurement devices, such as PMUs, will inform grid operators whether the system is operating within the physical grid limits. These constraints form the feasible set $\mathcal{S}_p$ to which the system variables must belong to heed steady-state physical grid requirements. Efficient coordination in the power grid entails the construction of the optimization problem $\mathcal{P}_c$

$$\begin{aligned} &\mathcal{P}_c : \min_x f(x) \\ &\text{s.t. } x \in \mathcal{S}_p, \end{aligned}$$

which consists of the cost function f; optimization variable x, which is a vector defined as $\{|V_i|, \theta_i, p_i, q_i \,|\, \forall\, i \in \mathcal{B}\}$; and the feasible set $\mathcal{S}_p$ that imposes physical constraints on these variables. The underlying characteristics of the objective function and feasible set composing $\mathcal{P}_c$ dictate the level of difficulty expected in solving the problem. Specifically, the objective function and feasible set must be convex for tractability [8]. Convex functions are defined as

$$\begin{aligned} &\theta f(x) + (1-\theta)f(y) \ge f(\theta x + (1-\theta)y) \;\forall\; x,y \\ &\quad \in \text{dom } f \;\forall\; \theta \in [0,1]. \end{aligned} \tag{12}$$

Intuitively, this definition can be interpreted as forming a linear line by connecting any two points x, y belonging to f and all points on that line must lie above or on that function for convexity to hold. In the power system, the cost of generation and demand is typically a quadratic function that satisfies the definition of convexity [9]. A set $\mathcal{S}_c$ is convex if

$$\alpha x + (1-\alpha)y \in \mathcal{S}_c \;\forall\; x, y \in \mathcal{S}_c, \forall\; \alpha \in [0,1]. \tag{13}$$

This definition can be intuitively interpreted as drawing a line connecting any two points in the set, and all points on this line must lie completely within the set. As nonlinear equality constraints, such as (6), that compose the set $\mathcal{S}_p$ do not satisfy this definition of convexity, $\mathcal{S}_p$ is not a convex set. If the feasible set is not convex, then solving the associated optimization problem will be NP-hard [10]. Thus, optimal grid coordination that accounts for exact physical constraints, such as power balance, becomes intractable very rapidly. Applying decomposition to this nonconvex problem for designing signals will result in local actuations that lead to system divergence and instability. Heuristic techniques can be applied to solve these [11]. However, no guarantees with respect to convergence or optimality can be established. Instead, simplifications or relaxations can be carefully applied to these relations to render the feasibility set $\mathcal{S}_p$ convex while retaining the defining characteristics of the physical grid. This convexification process allows for the tractable computation of the optimal solution with performance guarantees, which, in turn, allows for the construction of effective monitoring/control signals.

Traditional grid operations

The traditional electric grid has been designed to accommodate highly predictable power supply and demand. Thus far, grid operations have been well defined and mainly composed of contingency analysis, planning, and maintaining balance in demand/supply [3]. In contingency analysis, a

dynamic security assessment of the system is conducted where offline and online simulations are run to ensure that the grid operates within acceptable limits when various combinations of bulk synchronous generators are not operational [12]. Specifically, $N-1$ contingency is commonly upheld by grid operators to ensure that stability is maintained in the event that any one of the N generation systems in the grid fails. In this case, spinning reserves and ancillary services are commissioned to increase the stability margins during the recovery phase [13].

In planning operations, such as economic dispatch, generation supply is matched with forecasted demand in a cost-effective manner ahead of time (e.g., a day ahead). Power suppliers and distributors participate in day-ahead markets to sell and purchase electricity [14]. Both the suppliers and distributors use day-ahead forecasts of generation and demand for transacting in the market. In Canadian provinces, such as Ontario, bids are made, and an independent system operator will rank these bids and clear the market. The market-clearing price serves as the cost signals used in decisions governing the buying/selling power. No physical grid constraints are typically accounted for in this process [9]. Spot markets are based on similar principles but operate at a finer granularity (e.g., hourly schedules).

The degree of balance in power demand and supply dictates the system frequency in ac systems. Frequency control is maintained by generation sources at a much finer granularity (i.e., seconds to minutes) via primary, secondary, and tertiary control mechanisms [13]. Primary control mechanisms, which are typically employed in microgrid systems, focus on eliminating adverse effects due to transient events. Secondary and tertiary control mechanisms adjust the operating setpoint signals of generation systems to correct for deviations occurring over periods of minutes across various locations in the grid. These mechanisms are based on highly simplified real-power-balance equations that neglect the contributions of reactive-power and bus-voltage magnitudes. Other tertiary control mechanisms, such as AGCs located in the governors of synchronous generators, adjust mechanical power inputs via droop techniques (see the "Droop Control" section) to instantaneously adjust to changes in demands inferred using local measurement signals for maintaining nominal frequencies around acceptable thresholds.

Significant variability and wide margins of error in supply–demand forecast models of modern power entities prevent system operators from predicting well in advance reliable safety margins and an efficient balance of supply with demand.

These grid-operation processes have been highly effective until the recent proliferation of renewable generation sources, IPPs, and diverse power loads. Significant variability and wide margins of error in supply–demand forecast models of modern power entities prevent system operators from predicting well in advance reliable safety margins and an efficient balance of supply with demand. Using AGCs for frequency control is no longer sufficient, as this myopic technique cannot efficiently compensate for the considerable variability in power supply and demand introduced by renewables and diverse power consumers. Moreover, since lines are operating close to established limits, reactive-power and bus-voltage magnitudes are important considerations that can no longer be ignored in power-balance equations. Thus, the highly granular coordination of active power entities by designing signals based on realistic grid models is necessary to overcome these limitations.

However, as identified previously, incorporating exact physical grid relations, such as power-balance equations in the optimization formulation, leads to the nonconvexity of the feasible set $\mathcal{S}_p$. The distinguishing features of the system being coordinated must be leveraged to relax these nonlinear relations into convex constraints. These defining characteristics are unique in four specific counterparts of the power grid: TNs, DNs, microgrids, and power consumers. In the following, an overview is provided on how unique attributes in each one of these systems can be leveraged to simplify $\mathcal{S}_p$ while preserving important system characteristics.

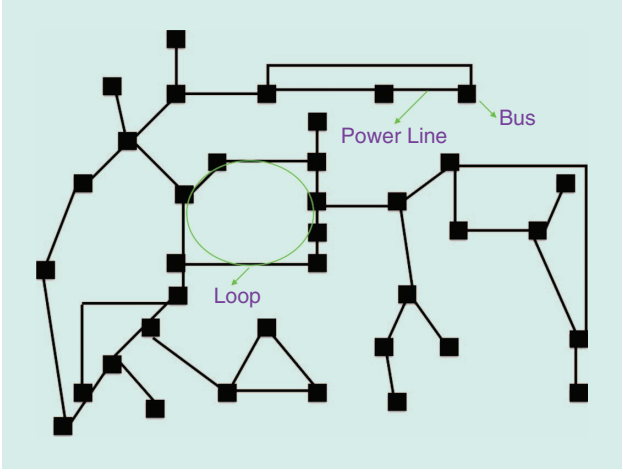

FIGURE 5. A simplified graphical representation of the IEEE 39-bus New England system [15].

TNs

TNs transport power across geographically dispersed regions that can span across hundreds of kilometers. All buses in a TN operate at high voltages to minimize excessive power losses that are typical in long lines. The ac power grid employs three separate phases for increasing conductor efficiency and safety. As all three phases in a TN are balanced, computations are based on single-phase constructs [3]. Thus, the TN topology can be represented as a connected graph where a single edge (power line) connects two nodes (buses). Figure 5 presents the simplified graphical representation of a TN consisting of 39 buses. A TN typically has a mesh structure, as loops or cycles can exist in the power network, as illustrated in Figure 5.

System operators typically apply approximations to TN power-balance equations based on three main assumptions: 1) bus voltage magnitude does not deviate from the nominal value $|V_i| \approx 1$ p.u.; 2) bus-angle differences are minor: $\theta_i - \theta_j \approx 0$; and 3) line admittance satisfies $|g_{ij}| \ll |b_{ij}|$. These lead to the dc power-flow equations that contain no ac terms and no voltage and reactive-power terms [3]

$$p_i = \sum_{j \in \mathcal{N}_i} -b_{ij}(\theta_i - \theta_j), q_i = 0 \; \forall \; i \in \mathcal{B}. \tag{14}$$

As the integration of unpredictable generation/loads threaten voltage stability, cause significant uncertainties in power actuation signals, and inflict congestions in the power lines [e.g., (10) and (11)], bus voltage and reactive power flow cannot be ignored in the TN and, thus, the dc power-flow equations are no longer representative of the TN.

With the introduction of EVs and other changes in the way consumers use power, DN bus voltages can dip to unacceptable values even during nonpeak periods.

Many proposals in the existing literature attempt to incorporate bus-voltage and reactive-power variables into the power-balance model while ensuring convexity [16], [17]. One specific example is the use of a first-order Taylor series to approximate the quadratic terms in (6) and a set of linear planes to estimate the $\cos(\theta_i - \theta_j)$ and $\sin(\theta_i - \theta_j)$ terms [18]. These changes transform the power-balance equations into a set of linear inequality constraints that retain the bus-voltage magnitude and reactive-power variables. The general form of the relaxed feasible set $\mathcal{S}'_p$ with these transformations in place is

$$\mathcal{S}'_p = \{Ax \leq B, Cx = D\},$$

where $A \in \mathbb{R}^{m \times n}, B \in \mathbb{R}^m, C \in \mathbb{R}^{k \times n}$, and $D \in \mathbb{R}^k$ encapsulate constant parameters associated with the physical grid and the related approximations. The general form of the relaxation is listed for the sake of brevity. These linear relations fairly accurately model power balance, as demonstrated in [18]. These approximations hold only in TN systems, not DNs, as assumptions, such as deviations in bus-voltage magnitudes, are small and will not be applicable. Thus, a different set of approximations must be applied in the DN setting.

DNs

DNs tap onto the bulk power supplied by the TN to provide power to local residential, commercial, and industrial consumers at lower voltages. The connection between the TN and a DN is established via a transformer substation that steps down voltage from the TN side. Thus, there exists a natural separation between the TN and DN. Power typically flows from the substation to individual consumers. As the DN operates at lower voltages, the voltage drops across these lines are not negligible. The physical network structure of the DN is radial (i.e., no loops), unlike the TN, as illustrated in the sample 33-bus Danish DN system presented in Figure 6.

Each DN is managed by an EPU, which forecasts local demands and supplies bids to the system operator to purchase power from day-ahead bulk-electricity markets [20]. The EPU bills power consumers using the advanced metering infrastructure, which consists of smart meters deployed at each consumer unit. The smart meter is capable of bidirectional communication and actuation. Typically, industrial/commercial consumers participate in demand–response programs, such as direct load control, where the EPU curtails power consumed by these entities as necessary during peak-demand periods via remote actuation signals to reduce stress on the system and provides adequate compensation for these disruptions [21]. Residential consumers participate in the time-of-use program in which different electricity prices are allocated at on-peak, midpeak, and off-peak periods that serve as indirect signals reflecting the congestion state of the grid [14]. These give consumers the incentive to use less power during peak periods.

With the introduction of EVs and other changes in the way consumers use power, DN bus voltages can dip to unacceptable values even during nonpeak periods. Also, microgeneration sources deployed by consumers inject surplus generation back into the DN. This results in reverse power flows that can lead to overvoltage conditions. These under- and overvoltage conditions make voltage less stable [i.e., (10)] and lead to equipment failure, the triggering of protection devices, and, ultimately, cascading failures that result in prolonged outages [4]. To prevent these calamities, systems need active DN coordination accounting for power balance and voltage stability by way of effective signal processing on grid-measurement data to reflect these conditions.

The exact power balance and voltage-limit constraints listed in (6)–(10) also apply to the DN. The simplification process is, however, not the same as that of the TN, as the physical attributes of the DN are substantially different. In fact, the three assumptions mentioned earlier obtain the dc power-flow equations in the TN do not hold for the DN. Much has been written about the relaxation of these constraints and about the following two widely used models. The first is the linear DistFlow model. In this model, nonlinear power losses (i.e., $I_{ij}^2 R$) in DN lines are ignored. The resulting drop in voltage magnitude in line $i - j$ can be modeled using the linear relation [22]

$$v_i - v_j = 2\,\mathrm{Re}(Z_{ij} S_{ij}), \tag{15}$$

where $v_i = |V_i|^2$ without loss of generality, the operator $\mathrm{Re}(\cdot)$ extracts the real component of the complex expression supplemented as the argument and Z_{ij} is the line impedance, which is the inverse of line admittance. The complex power flow on line $i - j$ is then modeled as

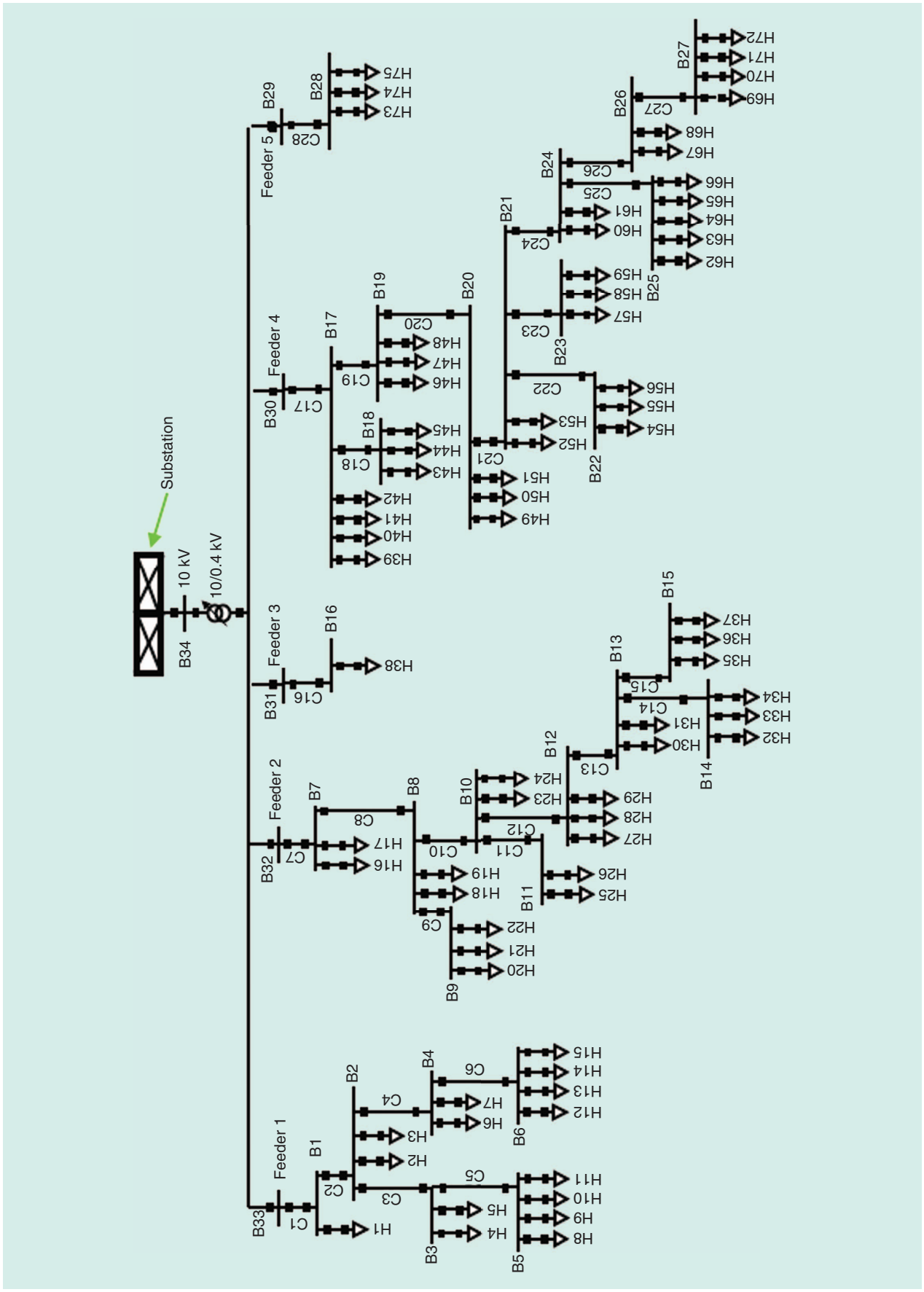

FIGURE 6. A graphical representation of the 33-bus Danish system [19].

$$S_{ij} = \sum_{k \in \mathcal{T}_i} S_k, \tag{16}$$

where j is the parent of node i (i.e., located closer to the feeder), $\mathcal{T}_i$ represents the subtree rooted at node i, and S_k is the complex power injection into bus k. This is a linear relation. Neglecting power losses in the DN enables a conservative estimation of voltage drop as these are strictly negative values in the power-balance equations. Relaxed feasible set has the form

$$S'_p = \{Ax \le B, Cx = D\}, \tag{17}$$

where A, B, C, and D are constant parameters.

The second model applies convex relaxations that transform the optimal coordination problem into semidefinite (SD) and/or second-order cone (SOC) programs [22]. The SOC $A \ge B$ relaxation converts the power-balance equations into convex quadratic inequality constraints

$$\mathcal{S}'_p = \{\| Ax + B \|_2 \le C^T x + D, Ex \le F, Gx = H\}, \tag{18}$$

where $A \in \mathbb{R}^{m \times n}$, $B \in \mathbb{R}^m$, $C \in \mathbb{R}^n$, $D \in \mathbb{R}$, $E \in \mathbb{R}^{k \times n}$, $F \in \mathbb{R}^k$, $G \in \mathbb{R}^{l \times n}$, and $H \in \mathbb{R}^l$ are parameters representing the relaxed physical grid attributes. SD relaxation introduces convex matrix inequality constraints in lieu of the original power-balance equality relations to obtain

$$\mathcal{S}'_p = \left\{ \sum_{i=1}^{k} A_i x \ge B, Cx \le D, Ex = F \right\}, \tag{19}$$

where $A \ge 0$ denotes that A is positive SD, and where $A > B$ denotes that $A - B \ge 0$, $B \in \mathbb{R}^{m \times m}$ and $A_1 \in R^{m \times m} \ldots A_k \in R^{m \times m}$ are matrices scaled by individual components of x.

These convex constraints obtained using SOC and SD relaxations are computationally more involved than the linear DistFlow equations. However, one major advantage is that, under certain conditions (e.g., radial structure and others) outlined in [23], these relaxations are exact in the DN. Thus, the tradeoffs between the linear DistFlow model and SD/SOC relaxations are the tightness of the relaxation versus computational efficiency.

Microgrids

Microgrids contain generation sources and consumers. Like the DN, these directly supply electricity to consumers and are typically deployed in remote communities. Microgrids can operate in grid-connected or islanded mode. In grid-connected mode, perturbations in demand/supply are absorbed by the main grid. In islanded mode, the microgrid, unlike the DN, is not connected to the main grid, and therefore, the inertia maintained by bulk-generation sources is no longer present. The microgrid will then need to be self-sufficient and use fast-acting signal processing and control mechanisms to stabilize the system during transient periods [24].

As transience can seriously undermine the stable operation of the microgrid, it is necessary to account for these in the power-balance relations. Capturing this transience in all three phases present in the system using ac variables is not straightforward due to the nonlinearities inherent in these sinusoidal variables. To overcome this difficulty, the $dq0$ frame of reference is used to convert the three-phase sinusoidal ac system states into 2D linear variables based on a rotating frame of reference [25]. The transience caused by the inductance and capacitance present in the lines and various power components is captured in the resulting linear ordinary differential equations in the microgrid

$$\dot{x}_{dq} = Ax_{dq} + B, \tag{20}$$

where, for notational simplicity, constant coefficients of the linear state variables x_{dq} are grouped into matrices $A \in \mathbb{R}^{m \times 2n}$ and vector $B \in \mathbb{R}^m$, and these represent the microgrid attributes. At the steady state, the differential terms will be 0, and the resulting equations are linear in terms of x:

$$Ax_{dq} + B = 0. \tag{21}$$

Thus, these linear equations are not only convex but also exact and incorporate all three phases. For the conversion from the three-phase abc to the $dq0$ domain, Park's transformation is applied. This is based on a common rotating frame of reference [3]. Every controller in the microgrid must maintain the same frequency and phase for the rotating frame. These values are generated by crystal oscillators present in these controllers and are synchronized by GPS signals communicated between these controllers [25].

The $dq0$ frame of reference converts power-balance equations into linear relations. However, when transforming other limits, such as voltage-magnitude constraints, into the $dq0$ frame, these become nonconvex relations. To overcome issues pertaining to nonconvexity, linear approximations can be applied in a manner similar to [18] to obtain

$$\mathcal{S}'_p = \{Ax_{dq} = B, Cx_{dq} \le D\}. \tag{22}$$

Power consumers

Power consumers are increasingly deploying storage systems, microgeneration systems (e.g., solar panels), and smart loads (e.g., EVs) in their premises, and these can be effectively coordinated by smart energy-management systems (EMSs) [26]. Storage devices and DG systems can be combined to reduce the amount of electricity purchased from the main grid. This promotes energy independence. When it is necessary to purchase power from the main grid or to conserve energy, smart appliances can be coordinated accordingly to maximize consumer comforts. The definition of user comfort is unique to each consumer and can vary based on diurnal patterns, seasons, and weather conditions. User comfort is associated with the tolerance $\bar{P}_j^r$ to change at various coordination horizons [27]

$$0 \le P_j^r \le \bar{P}_j^r, \tag{23}$$

where P_j^r represents the reduction in power demand by consumer j. Energy budgets E_j^d representing the maximum amount of energy reduction tolerated by the consumer will ensure that energy is not cut too much:

$$E_j^r + \Delta t P_j^r \leq E_j^d, \tag{24}$$

where E_j^r represents energy reductions so far during the day, and Δt is the length of the current coordination interval. Power reduction is typically discrete as appliances function at specific power levels or operate in a binary fashion (i.e., on/off). Hence, $P_j^r \in \mathcal{D}_j$, where $\mathcal{D}_j$ represents a discrete set of power-reduction values. These are combined to construct the feasible set

$$\mathcal{S}_p = \{Ax = B, Cx \leq E, x \in \mathcal{D}\}, \tag{25}$$

where A, B, C, and E are constant parameters. Discrete variables introduce nonconvexity. However, game theoretic constructs can be applied to overcome issues due to discreteness, as is discussed later in this article.

Summary of physical grid models

Realistically modeling the underlying electrical characteristics of the power grid is a vital step in building an efficient grid-coordination framework based on signal processing. The grid model must allow for tractable computations while maintaining important physical attributes of the system. The simplification processes presented for the four main components of the power grid have resulted in the system models summarized in Table 1. Usually, in the selection of the underlying grid model, the main tradeoffs are between computational complexity and tightness of the relaxations (i.e., representation of the original constraint set).

Now that the physical grid constraints can be incorporated in a tractable manner into the optimization framework, the next step will be to explore how signals and actuation can be designed to enable intelligent actuating nodes to adaptively make the best actuation decisions.

Table 1. A summary of physical power-balance constraints.

System	Model of Power Balance	Complexity of Terms	Tightness
TNs	dc power flow	Linear	Weak
	Linear ac approximations	Linear	Tight
DNs	Linear DistFlow	Linear	Tight
	SOC relaxations	Quadratic	Exact
	SD relaxations	Positive SD	Exact
Microgrids	ac power flow	Sinusoidal	Exact
	*dq*0 frame	Linear	Exact
Power consumers	Comfort requirements	Linear	Exact
	Appliance actuation	Discrete	Exact

Decision-making topologies

Decision-making topologies govern the way actuating power entities exchange information and use externally/locally generated signals to determine choices. These intelligent actuation processes must foster greater efficiency in the system while heeding physical infrastructure constraints. Thus, key elements of the decision-making process are 1) the effective construction of signals that succinctly capture relevant information about the operating status of the system; 2) the manner in which signals are exchanged among participating nodes; and 3) effective processing of these signals for feasible and efficient decisions. Four different types of decision-making topologies are presented in this section, and these are based on centralized, decentralized, distributed, and independent coordination paradigms. The suitability of each one of these coordination constructs depends on the application (e.g., planning, preventative actions, efficient power balancing, and others) and system characteristics (e.g., TN, DN, microgrid, and others).

Decision-making topologies govern the way actuating power entities exchange information and use externally/locally generated signals to determine choices.

Centralized coordination

Centralized coordination consists of a single management entity (e.g., a system operator) that computes the proper operation setpoint signals for each actuating entity present in the system [3]. To incorporate physical infrastructure limits into the computations, the management entity must be aware of detailed nuances associated with the physical topology (e.g., connection structure of nodes, node/line attributes, actuation limits, and others) of the entire system. This significantly limits flexibility in the system, as the central controller must be aware of every change taking place throughout coordination domain. To centrally solve the coordination problem in a tractable manner, appropriate relaxations depending on the system being coordinated can be applied to the feasible set $\mathcal{S}_p$, as discussed in the previous section, to render the $\mathcal{P}_c$ convex. Then, well-known convex solvers can be used to solve the relaxed problem in polynomial time $O(n^p)$, where n represents the number of entities being coordinated [8].

Extremely powerful computational resources, such as cloud-computing platforms, can be used to centrally compute the best solution to the convex coordination problem [28]. The main issues with this setup are threefold: 1) highly fluctuating grid parameters; 2) the risk of data exposure; and 3) the single point of failure. Since grid parameters, such as generation capacities and demand patterns, cannot be accurately predicted using long-term models, the central coordinator must accrue these values directly from the varying nodes over short intervals [29]. These data signals sent by individual nodes will result in the establishment of n dedicated communication links with the central controller. This information must be processed to compute the optimal setpoints, which are then conveyed individually to every actuating node by the coordinator. This necessitates the forging of n more dedicated communication links in the reverse direction. Hence, at every

coordination period, $2n$ point-to-point links are established to exchange measurement and actuation signals. When there are thousands of highly varying nodes in the system (e.g., TN or DN), the ensuing overheads become excessive, as summarized in Table 2, where k, k_1, k_2, and p are constants.

Moreover, these frequently exchanged signals processed at a central location can be easily intercepted via cyberchannels. In this case, highly revealing information about the grid and its operating trends can be gleaned by an adversary and be exploited to perpetrate an insidious cyberphysical attack on the system [30]. To address these security issues, additional layers of encryption can be added to the data being exchanged. This can, however, impose greater overheads to the already resource-intensive centralized coordination process. Also, if the central entity coordinating the entire system is not functional, then this single point of failure can undermine the operation of the entire system.

Central coordination is not suitable for controlling a vast system with many nodes. As it is not very scalable, central coordination is more suited in a smaller and contained setting, such as for a home or building or over long control horizons.

Table 2. A summary of overheads in centralized coordination.

System	Nodes n	Complexity Computational	Communication
TNs	1,000	$O(n^p) \approx k_1 1{,}000^p$	$O(n^2) \approx k_2 1{,}000^2$
DNs	1,000	$O(n^p) \approx k_1 1{,}000^p$	$O(n^2) \approx k_2 1{,}000^2$
Microgrids	10–100	$O(n^p) \approx k_1 100^p$	$O(n^2) \approx k_2 100^2$
Power consumers	10–20	$O(k^n) \approx k_1^{20}$	$O(n^2) \approx k_2 20^2$

Distributed coordination

In distributed coordination, actuation decisions are made locally by every active node instead of by a central entity. These decisions depend on external signals communicated periodically. Unlike decentralized coordination, the distributed coordination process involves a central entity that provides general information to actuating nodes in the form of broadcast signals computed using aggregate monitoring data encapsulating global system trends.

Extremely powerful computational resources, such as cloud-computing platforms, can be used to centrally compute the best solution to the convex coordination problem.

For example, in the DN, the EPU is a central entity that manages all of the electricity billing processes and, thus, has access to information generated by smart meters [20]. This information can be aggregated by data concentrators in a manner that reveals the general state of the DN with respect to voltage stability, load balancing, costs incurred, sustainable power consumption/generation, and so on. General trends inferred from this information are then broadcast by the EPU to individual actuating elements (e.g., power consumers, micro-DGs, storage systems, and so on), which can then respond adaptively to increase system efficiency while heeding local constraints. The EPU does not need to form dedicated point-to-point communication links, as the information broadcast is common to all entities in the system. The issue of concentrated computation is also resolved, as this is offloaded to individual actuating agents that act in parallel. Two approaches based on dual decomposition and population game (PG) theory illustrate the effectiveness of the distributed coordination paradigm.

Dual decomposition

In the first approach, signals constructed by the central aggregating entity aim to establish a balance in the overall power demand and supply in the system. The design of these signals is illustrated via two different approaches: 1) the subgradient (SG) method and 2) the water-filling technique. Every actuating node i (e.g., storage systems, DGs, and others) has its own definition of cost $f_i(x)$ and, hence, the objective of the coordination problem is separable. Power-generation capacities and other constraints particular to each active node i form the local feasible set $\mathcal{S}_i$. The only binding constraint is the global balance in demand and supply:

$$\mathcal{P}_{ED}: \min_{x_i \in \mathcal{S}_i} \sum_{i=1}^{n} f_i(x_i)$$
$$\sum_{i \in \mathcal{G}}^{n} A_I^T x_i - \sum_{i \in \mathcal{D}}^{n} A_I^T x_i = 0,$$

where x_i represents the optimization variables pertaining to node i, and the sets $\mathcal{G}$ and $\mathcal{D}$ represent nodes that generate power and consume power, respectively. The variable set in $\mathcal{D}$ remains constant in economic dispatch problems as the generation setpoints of variables in $\mathcal{G}$ are optimized based on the associated cost and overall demand in the system. When demand response is considered, power consumption by flexible consumers in $\mathcal{D}$ is adjusted to meet the overall power injected into the system via generation sources. The value A_I serves as an indicator vector for notational convenience that selects the real power p_i variable from the set x_i. It is assumed that both the demand and supply variables are continuous. The dual problem is then constructed by formulating the Lagrangian in which the dual variable ν associated with the binding constraint is introduced [8]:

$$\mathcal{P}_{ED}^{D}: \max_{\nu \in \mathbb{R}} \min_{x_i \in S_i} \sum_{i=1}^{n} f_i(x_i) - \nu \left(\sum_{i \in \mathcal{G}}^{n} A_I^T x_i - \sum_{i \in \mathcal{D}}^{n} A_I^T x_i \right).$$

In the SG method, the dual problem is decomposed by grouping optimization variables associated with each actuating node together to form the local optimization problem [31]:

$$\mathcal{P}_{ED}^{S}: \min_{x_i \in S_i} f_i(x_i) - \nu(\mathbb{I}_G(i) A_I^T x_i - \mathbb{I}_D(i) A_I^T x_i),$$

where $\mathbb{I}_G(i)$ is an indicator function that returns one if node i is a generation source and zero otherwise. The value $\mathbb{I}_D(i)$, defined in a similar manner, is used to identify whether node i is a power consumer. The variables ν and x are computed

iteratively by the central aggregating entity and individual nodes. The central aggregating entity computes ν by fixing x to the current value taken in the system at time t in $\mathbb{P}_{ED}^{D}$. This value ν is broadcast to individual agents, which then substitute this into the variable ν to compute x_i by solving $\mathcal{P}_{ED}^{S}$.

Thus, the original problem is divided into master and slave problems where, in the master problem, the central coordinating entity attempts to iteratively compute ν via the SG update technique, where $q(\nu)$ is the SG of the master problem at point ν when x_i is fixed and α is the step size [32]:

$$\nu_{t+1} = \nu_t + \alpha q(\nu_t). \tag{26}$$

The SG turns out to be the difference in aggregate generation and demand at time t:

$$q(\nu_t) = \sum_{i\in\mathcal{D}}^{n} A_I^T x_i^t - \sum_{i\in\mathcal{G}}^{n} A_I^T x_i^t, \tag{27}$$

and this is an aggregate measure that can be easily obtained from data concentrators. This value is broadcast by the central aggregating entity in a periodic manner (e.g., every second).

In the slave problem, each actuating node computes the optimal value of x_i, which is a function of ν_t and local constraints $\mathcal{S}_i$. Since $\mathcal{P}_{ED}$ is convex, these iterative revisions are guaranteed to converge [33]. However, the step-size α must be customized for the system under consideration to avoid oscillatory behavior, as illustrated in Figure 7, where the total demand is fixed and local generation systems adaptively actuate the real-power injection to match this demand. The coordination occurs during every 10-min interval, and the system consists of 20 large-scale renewable sources with highly fluctuating generation capacities. Clearly, these individual sources are able to rapidly converge to the best solution for the appropriate step size.

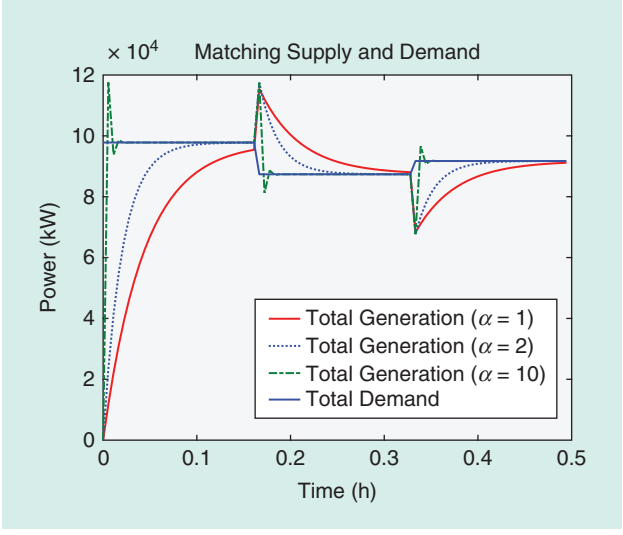

FIGURE 7. The impact of α on convergence using the SG method.

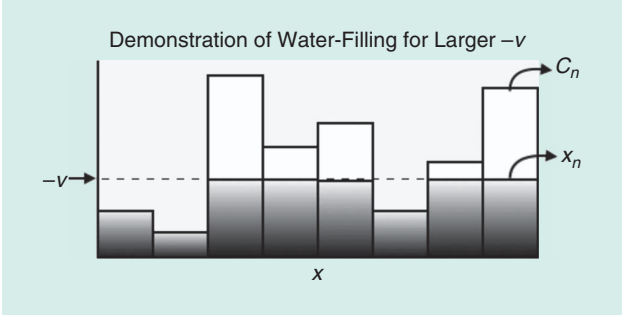

FIGURE 8. A water-filling analogy [34].

Alternatively, $\mathcal{P}_{ED}^{D}$ can also be solved using the water-filling method [34], where the central coordinating entity computes ν iteratively using binary search and the stopping criteria $\sum_{i=1}^{d} x_i^d - \sum_{i=1}^{g} x_i^g = 0$. Individual agents, on the other hand, receive ν_t broadcast by the aggregator and analytically compute local actuation by applying the Karush Kuhn Tucker optimality conditions, which are necessary and sufficient in convex optimization problems [8].

First-order optimality is expressed as

$$\frac{\partial L(x^*, \nu^*)}{\partial x_i} = 0.$$

Primal and dual feasibility is expressed as

$$x^* \in S_p, \nu^* \in \mathbb{R}.$$

Complementary slackness is expressed as

$$\nu^*(\mathbb{I}_G(i)A_I^T x_i^* - \mathbb{I}_D(i)A_I^T x_i^*) = 0,$$

where L is the objective of the dual problem $\mathcal{P}_{ED}^{D}$, and x^* and ν^* are optimal values of the problem. This method is called the *water-filling method,* as the local constraints, such as generation capacity c_i, form a boundary analogous to an enclosure, as illustrated in Figure 8. The water level represented by $-\nu$ reflects the aggregate state of the system and, this is increased until the stopping criteria is met (i.e., demand is equal to supply), at which point, the optimal solution x^* is achieved. Like the SG method, the convergence of the system to this optimal point depends on how ν is updated. With the binary search method, oscillations will be present. Also, the convergence rate of both methods is proportional to the number of nodes in the system $O(n)$ [33]. Thus, the three main issues associated with the SG and water-filling methods are as follows: 1) actuation is based on a continuous domain (e.g., smart appliances operate in discrete power levels); 2) smooth convergence entails fine-tuning of the updating parameters; and 3) convergence time depends on the number of nodes being actuated.

PG theoretic approach

Introducing discrete variables can render $\mathcal{P}_c$ an NP-hard problem [10]. When there are thousands of discrete variables involved (e.g., in DNs with thousands of appliances), solving the problem as is becomes impractical, as NP-hard problems are not scalable or tractable. Instead of directly solving $\mathbb{P}_c$, applying a PG theoretic approach to transform this problem into a

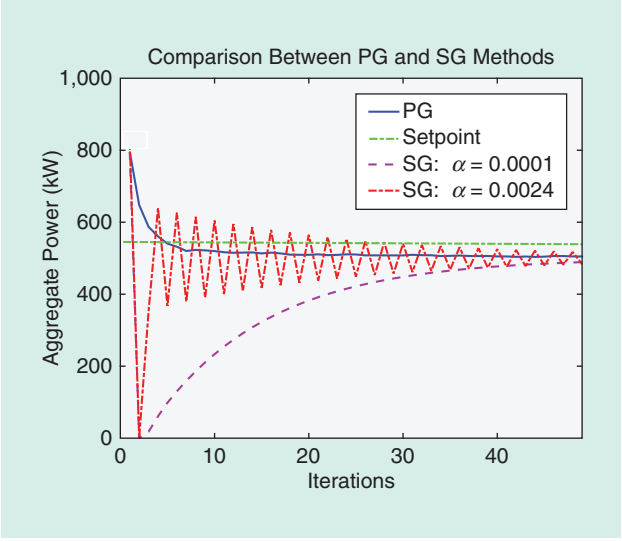

FIGURE 9. A comparison between the PG and SG methods.

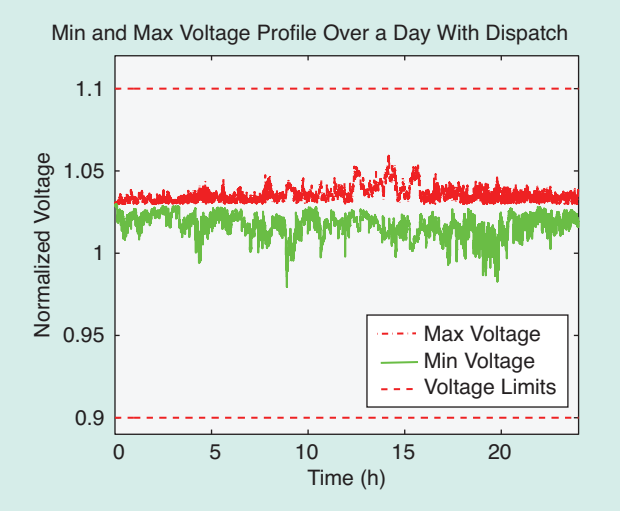

FIGURE 10. The bus-voltage magnitudes with a feasibility check. Min: minimum; Max: maximum.

game consisting of thousands of players equipped with discrete strategy sets resolves many of the previously mentioned issues, as discussed later in this section [35]. The main premise behind the PG approach is that, when one player switches strategies, the effect on the overall system cost is incremental. If individual strategy revisions are made so that the overall potential/cost of the system decreases over time, then an equilibrium state will be reached eventually [36].

All possible discrete strategies available in the system form the set $\mathcal{Y} = \{y_1, \ldots, y_m\}$, where y_i represents the discrete power level associated with strategy i. The central aggregating entity maintains another variable $\mathcal{Z} = \{z_1, \ldots, z_m\}$, where z_i is an aggregate variable that represents the fraction of agents in the population that are using strategy i. Thus, $\mathcal{Z}$ is a continuous variable defined over a convex simplex [37]:

$$\mathcal{Z} = \left\{ z \in R^m \mid \sum_{i=1}^{m} z_i = 1, z_i \geq 0 \; \forall \, i \in m \right\}. \tag{28}$$

This variable substitution can be applied to $\mathcal{P}_{ED}^{D}$, and this transformed problem is referred to as $\mathcal{P}_{ED}^{Z}$ with an objective $L(\nu, \mathcal{Z})$. The central coordinating entity can now directly solve this dual problem to obtain ν^* and $\mathcal{Z}^*$. The main challenge now lies in achieving this optimal distribution $\mathcal{Z}^*$ in the population. Every agent may have different local operating conditions and constraints that the central coordinating entity does not yet know. Thus, instead of directly actuating individual agents, the coordinator computes the gradient of $\mathcal{P}_{ED}^{Z}$ with respect to each strategy to obtain $\partial L / \partial z$ and broadcasts this gradient vector to all agents in the system.

The agents will revise their local actuation strategy at a randomly selected time in a manner that accounts for local constraints and moves the aggregate state of the system in the opposite direction of the gradient. This process will be repeated until there is no incentive to switch (e.g., gradient is 0). At this point, Nash equilibrium is achieved, and the distribution $\mathcal{Z}$ in effect is the optimal solution for $\mathcal{P}_{ED}^{Z}$ [35]. This can be proven by showing that the system dynamics ensuing from these incremental revisions has a Lyapunov function, which is exactly $L(\nu, \mathcal{Z})$. The existence of a Lyapunov function guarantees convergence to $\mathcal{Z}^*$, which is the point that results in the gradient of the Lyapunov function being zero (i.e., $\partial L / \partial z = 0$) [35]. This is also the condition for first-order optimality, which implies that $\mathcal{Z}^*$ is the solution of $\mathcal{P}_{ED}^{Z}$. The convergence speed of this method is independent of the size of the system, as aggregate measures compose the variable set.

Figure 9 compares the convergence of a system composed of 1,000 nodes representing smart appliances over a single coordination period of 1 min via the PG and SG methods. Realistic demand models, appliance usage statistics, and penetration rates have been employed for these simulations. At each iteration, the central aggregating entity broadcasts a signal to the actuating nodes. With the SG method, it is assumed that the actuation (i.e., demand curtailment) is continuous. With the PG theoretic method, more realistic discrete strategies are used instead. The PG theoretic method displays fast convergence and exhibits no oscillations. This is not the case with the SG method when $\alpha = 0.0024$. Although the PG theoretic method is highly effective for large-scale discrete coordination, it cannot be applied to systems consisting of a few nodes, as the stochastic nature of the random decision-making process will take effect and introduce

Table 3. A summary of distribution decision-making topology.

Coordination Component	System	Convergence
Aggregating signal	SG	$O(n)$
	Water filling	$O(n)$
	PG	$O(\lvert \mathcal{Y} \rvert)$
Local feasibility check	Tree network	$O(d)$
	Mesh network	$O(n)$

perturbations. This is eliminated in a system consisting of many participants due to the strong law of large numbers.

Local feasibility checking

So far, three methods have been presented for designing signals broadcast by the central aggregating entity in the distributed setting. Active nodes factor these signals into selecting appropriate local actuation. Prior to implementing the computed actuation, the node proceeds to evaluate whether or not the actuation strategy at hand violates local capacity limits and/or infrastructure limits. Local capacity limits are embedded into the computation of the actuation signal via the SG and water-filling methods. With the PG method, discrete strategies that violate local capacity limits are not considered as candidates for strategy revision. Infrastructure limits, such as bus-voltage and apparent line limits, are taken into account by way of communication with neighboring nodes.

In the DN or microgrid, which has a radial topology, an actuating agent selects a random time for making the strategy revision so that its strategy change does not coincide with other nodes in the system. At this time, this node communicates with bus agents residing in its local feeder branch to ascertain that the impending change in power flow will not violate bus-voltage magnitudes or apparent power-flow limits (e.g., using DistFlow equations) [38]. The communication complexity of this process is $\mathcal{O}(d)$, where d is the depth of the tree representing the DN rooted at the substation. Figure 10 illustrates the maximum and minimum voltages in the 33-bus DN with this local feasibility check in place for the PG-based distributed coordination [19] composed of 1,000 active nodes. Bus-voltage magnitudes are within acceptable limits of $\pm 10\%$.

In the TN, which has a mesh topology, this can be verified via repeated exchange of local state signals with neighboring nodes. Specifically, the alternating direction method of multipliers (ADMMs) can be used to evaluate whether infrastructure constraints are violated, as discussed in the section "Decentralized Coordination." The complexity of this process is $\mathcal{O}(n)$ [39]. If the impending strategy revision violates infrastructure limits, the revising agent will not proceed with the computed change in actuation.

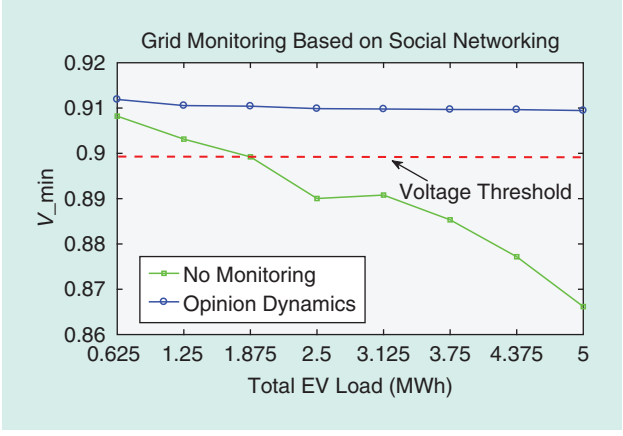

FIGURE 11. The integration of EVs with monitoring based on social networking.

Summary of distributed coordination

In the distributed coordination technique, a central aggregating entity informs participating nodes of the global trends in the system via periodic broadcasts of the generalized signals. Agents use these signals to make local strategy revisions while also accounting for local infrastructure limits. These signals are designed using aggregate measures (e.g., a surplus/deficit in demand/supply, the proportion of agents using a particular solution, and so on), which are readily available via data concentrators and supervisor-control and data-acquisition systems. Convergence properties are analyzed using convex optimization techniques (e.g., SG and water-filling methods) and control theory (e.g., Lyapunov functions). Table 3 presents a summary of the performance characteristics of these distributed decision-making systems.

This distributed coordination paradigm naturally fits into systems, such as DNs, as there is a central entity, such as an EPU, that has readily available access to aggregate measurements in the system. Moreover, the radial structure of the DN allows for localized checks of physical power-balance constraints. However, this technique will not be appropriate in deregulated systems, such as TNs consisting of independent entities (e.g., IPPs) that are not centrally managed. In these cases, a completely decentralized solution where no central aggregating entity is present is suited for establishing coordination among these independent elements.

Decentralized coordination

In decentralized coordination, individual actuating entities iteratively exchange signals with nearby nodes to make local decisions. As no central entity is involved in directly actuating or coordinating nodes, no single node needs to be aware of the entire physical network structure or needs to gain access to aggregate data sets. This aligns with the deregulated nature of the modern power grid and eliminates single-point-of-failure issues. In the presence of malfunctioning power devices, normally operating nodes can infer these anomalies via signals exchanged among each other and adaptively modify local actuation to isolate these issues and reestablish the nominal operation of the system. In the power engineering literature, the three common coordination techniques for the decentralized coordination of demand and/or supply are the consensus method, ADMM, and potential games. Extensions of these techniques are used in applications related to grid monitoring, power balance, and preventative actuation.

Consensus method

In the consensus method, all participating agents repeatedly exchange information with one another to reach an agreement (e.g., total demand is equal to total supply). Convergence to the average consensus is proportional to the largest eigenvalue of the Laplacian matrix representing the information exchange network topology [40]. This notion of consensus is also used for inferring trends in social networking platforms, which can be applied in the grid context for monitoring processes [41].

Every node in the power grid can have an opinion $s_i(t)$ about the operating state of the power grid at time t. This opinion can be exchanged repeatedly among immediate neighbors until an equilibrium is attained. DeGroot's method, which entails the computation of myopic averages by individual nodes, is typically applied in this context. As such, the evolution of opinions (i.e. opinion dynamics) over time via this method can be modeled as

$$s(t) = A_d s(t-1), \tag{29}$$

where A_d is the adjacency matrix representing the underlying topology of the communication network, and $s(t) = \{s_1(t) \cdots s_n(t)\}$ is the vector containing the opinion of all n nodes at discrete time steps t. This refinement of opinions via DeGroot's method will eventually converge to the global average of the opinions in the network as long as the communication network is fully connected. This global average can be used to deduce the state of the network (e.g., congested, stressed, healthy, and so on), which enables individual agents to adaptively respond to improve the general health of the system.

In Figure 11, this social networking method has been applied to determine the connection of EVs to the grid for charging purposes in a 128-bus DN system. With this decentralized monitoring in place, it is clear that dangerous voltage violations due to congestion can be prevented.

ADMM approach

Establishing optimal power flow via the ADMM approach entails the design of signals that incorporate information about local infrastructure states (e.g., the apparent power-flow and bus-voltage magnitude) by every actuating node. These signals are then exchanged with the nodes of direct neighbors and used to refine local actuation to increase efficiency while maintaining locally inferred feasibility. Signals are repeatedly exchanged with peers until a global consensus regarding the nominal operation of the entire system is attained.

The design of signals is composed of two steps. First, the nonconvex power-balance relations are converted into a set of convex constraints via one of the linear ac approximations, convex relations via SD/SOC, or steady-state $dq0$ transformation, as listed in the section "Tractable Physical Grid Modeling." The next step will be to decompose these power-balance equations for each node to infer local feasibility. However, as power balance depends on power flowing from directly connected nodes, it is not possible to directly decompose this for individual buses. To render the power-balance equations separable, each node maintains three different sets of variables [39]. The first set x_i contains local variables pertaining to the actuating node (e.g., local generation, local voltage magnitude, and so on). These variables are subject to local constraints $\mathcal{X}_i$. The second set of variables are the perspectives y_{ij} maintained by node i of variables belonging to all neighboring nodes $j \in \mathcal{N}_i$, which are subject to constraints $\mathcal{Y}_i$. These constitute the local problem $\mathcal{P}^i_{\text{ADMM}}$:

$$\mathcal{P}^i_{\text{ADMM}}: \min_{x_i \in \mathcal{X}_i, y_i \in \mathcal{Y}_i} f_i(x_i)$$
$$x_j = y_{ij} \; \forall \; j \in \mathcal{N}_i.$$

The third set of variables ν_{ij} are the Lagrangian multipliers associated with the consensus constraint between the actual and perspective variables as listed in $\mathcal{P}^i_{\text{ADMM}}$. The goal of every node will be to attain consensus (i.e., $x_j - y_{ij} = 0 \; \forall \; j \in \mathcal{N}_i$) between the perspective y and actual x variables where ν_{ij} indicates the degree of mismatch.

This can be achieved by first constructing the augmented Lagrangian $L_\rho(x, y, \nu)$ of $\mathcal{P}_{\text{ADMM}}$ that contains an additional term squaring the mismatch between the perspective and actual variables. This term is weighted by a positive constant ρ. Then, the iterative ADMM updating technique is applied to the associated variables as [42]:

$$x^{k+1} = \operatorname*{argmin}_x L_\rho(x, y^k, \nu^k),$$
$$y^{k+1} = \operatorname*{argmin}_x L_\rho(x^{k+1}, y, \nu^k),$$
$$\nu^{k+1} = \nu^k + \rho(x^{k+1} - y^{k+1}).$$

This process entails the exchange of three different sets of parameters with neighboring nodes at each updating iteration k. These sets of parameters are guaranteed to converge if $\mathcal{P}_c$ is convex. This is indeed the case when convex relaxations are applied to the power-balance relations. Furthermore, the convergence rate is proportional to the number of nodes n in the system [i.e., $\mathcal{O}(n)$]. Figure 12 shows the ADMM method applied in the TN setting using the linear ac approximation of power-balance constraints and the change in the residual (i.e., $\|x - y\|_2$) over one coordination interval of 10 min. Signals are exchanged every 6 s. This system is composed of 2,736 buses [15], and it is clear from Figure 12 that the decentralized coordination mechanism results in fast convergence to the optimal solution. Thus, the communication of signals to neighboring nodes that contain current values computed for local, perspective, and dual variables enables every node to adaptively respond to changes in the system in a decentralized manner while accounting for physical power-balance relations.

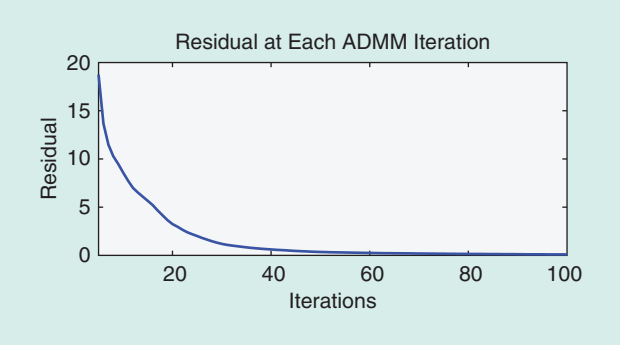

FIGURE 12. Optimal power-flow coordination via ADMM in the Polish 2,736-bus system.

Potential game approach

Decentralized coordination can also be applied in preventative measures where build-up of congestion/stress can be detected and individual agents can actuate to avoid potential cascading failures. For instance, the physical network topology in the DN is typically fairly static. Individual switches can be activated to add or remove lines to reconfigure the system topology in case of line outages and other emergencies. These switches are typically reconfigured in the aftermath of an event not a priori. With the proliferation of EVs and highly variable renewable loads, loads across the DN feeders can be unbalanced and voltage drops across lines can be excessive. The bus switches can be activated to achieve a more efficient topology and reduce the risk of failure

This topology reconfiguration problem consists of discrete variables (e.g., a switch or no switch) that render the problem very difficult to solve directly. A decentralized algorithm based on the potential game approach enables every bus switch to decide whether to shift to a new node by communicating with neighboring peers and, thereby, identifying the impact of the switch on power balance (e.g., modeled using linear DistFlow equations) in the network. These decisions are sequential, and the topology resulting from a switch at time t is denoted as $\mathcal{T}_t$. These sequential decisions improve the voltage profile $V(\mathcal{T}_t)$ of the network [43]:

$$V(\mathcal{T}_0) > V(\mathcal{T}_1) > V(\mathcal{T}_2) > \cdots \tag{30}$$

As the set of strategies available to each switching agent is finite, this sequence will converge within finite time to a Nash equilibrium in which no agents shall regret their current state (i.e., it is not possible to deviate further without incurring additional costs). These repeated revisions of discrete strategies will result in the optimal topology configuration if discrete concavity conditions are met [44]:

$$\max_{x,y,z\in X:\|x-z\|=\|y-z\|=1} U(z) = \begin{cases} > \min\left(U(x), U(y)\right), U(x) \neq U(y) \\ \geq U(x) = U(y), U(x) = U(y) \end{cases}, \tag{31}$$

where X is a set consisting of all configurations of individual switches and x, y, and z are vectors that belong to this set X in which the ith element is zero if switch i is connected to the original node and one if it is connected to the new node. The value U is the utility function that depends on the current state of switches in the system. Typically, heuristic algorithms are used for this purpose, and these have no guarantees on convergence and optimality. Figure 13 illustrates the effectiveness of the potential game approach for DN topology reconfiguration in comparison to the heuristic fast nondominated sorting genetic algorithm (FNSGA) [45]. In this figure, $\mathcal{I}$ indicates how close the result from applying the algorithms is compared to the optimal voltage profile computed using the brute-force method, which applies load-flow analysis using MATPOWER. On the x axis, the tuple $69-5$, for example, models a 69-bus DN consisting of five switches. Clearly, the potential game approach yields far better results than the heuristic technique.

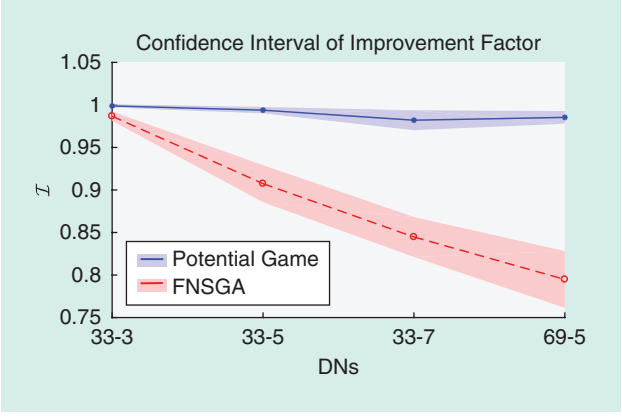

FIGURE 13. A comparison of the performance of DN topology reconfiguration algorithms.

Table 4. A summary of decentralized algorithms and applications.

Method	Application	Convergence
Consensus	Grid monitoring	$O(n)$
ADMM	Power balance	$O(n)$
Potential game	DN topology reconfiguration	$O(k)$

Summary of decentralized coordination

Decentralized coordination enables individual agents, by exchanging signals with neighboring nodes, to adaptively respond to changes and perturbations and, thereby, progressively improve the global state of the system while adhering to local constraints. Table 4 summarizes the three decentralized methods and applications for adaptive and proactive actuation that have been presented.

Independent coordination

In all of the coordination paradigms presented earlier, the nodes communicate. The communication channel is subject to latencies in the order of milliseconds [46]. In certain applications that require fast-acting control and response, this latency will not be tolerable (e.g., primary control) [24]. In these scenarios, only local measurements (e.g., bus-voltage magnitude, current, frequency, and so on) can be used by actuating nodes for inferring the general state of the system, and actuation is, therefore, independent of external input. Specific actuation mechanisms include those based on droop control, primal-dual dynamics, and machine-learning techniques.

Droop control

Droop control is widely used in both TN and microgrid settings by generation systems that measure local frequency deviations to infer the degree of mismatch in demand/supply in the system [3]. If there is higher power demand in comparison to

the supply in the system, generation frequency will decrease and, thus, more real power must be put out by the generator and vice versa when the demand is lower than supply. To maintain the frequency of the system around nominal values, the generator controller uses the relation [3]:

$$\omega = \omega_{\text{ref}} - k_p(P - P_{\text{ref}}), \tag{32}$$

where k_p is the droop coefficient constant associated with real load sharing, and ω_{ref} and P_{ref} are the reference frequency and reference active power setpoint computed by solving an economic dispatch problem, respectively. If the locally measured frequency decreases to ω, then active power P is increased to the value obtained by solving (32). This droop control mechanism allows for active power sharing among multiple generation units in the event of minor disturbances or deviations of demand/supply from forecasted values. These myopic actuation decisions are especially suited for systems that do not experience significant deviations from forecasted values. However, with the recent proliferation of renewables and high-power consuming devices, these myopic decisions will not be efficient, as these will attempt to maintain setpoints that are unrepresentative of the actual conditions in the system.

Primal-dual dynamics

To ensure that actuation computed using local measurements is optimal in a simplified context, recent work on primal-dual dynamics capitalizes on problem formulations, such as $\mathcal{P}_{ED}$, to use local frequency and power-flow measurements to iteratively compute the optimal actuation for addressing this problem. First, a dual variable ν for the overall balance in power demand and supply is introduced. This variable ν_i is maintained locally by every node. At optimality, ν_i maintained by node i must be equal to the ν_j maintained by node j. Another dual variable π_{ij} is introduced to represent this synchronization of ν among nodes i and j. The work in [47] proved the equivalence of ν_i with local frequency ω_i and π_{ij} with power flow P_{ij} from node i to j based on the simplified linear dynamical equation of power flow:

$$\Delta\dot{P}_{ij} = B_{ij}(\Delta\omega_i - \Delta\omega_j), \tag{33}$$

where B_{ij} is a constant derived using nominal bus voltages and line reactance. Thus, since these variables can be measured locally, there is no need to broadcast these dual variables to actuating nodes, as actuation updates can be performed using these local measurements. Although this method allows for the establishment of optimality with respect to simplified dispatch or load control for frequency control, it does not account for reactive-power and bus-voltage magnitudes, which are important constituents in decision making in the modern power grid.

Machine learning

Machine learning is currently a prevalent area of research and is widely applied in the context of droop control for voltage stability. Voltage magnitude $|V_b|$ of bus b must lie within the 1 ± 0.1 p.u. threshold for the nonfaulty operation of power components. At the extreme ends of this spectrum, when $|V_b|$ is 1.1 p.u., generation is excessive in comparison to demand and, when $|V_b|$ is 0.9 p.u., demand is much higher than generation. The work in [48] divides the interval $[0.9, 1.1]$ into subintervals, where each subinterval represents an operation mode. Based on the operation mode at hand, actuating grid elements, such as storage systems, DGs, and loads, actuate at three modes: maximum power draw/injection, voltage control, minimum power draw/injection. These operational and actuation modes are derived via machine-learning concepts such as fuzzy-logic techniques. Other adaptive controllers, such as those using model predictive control techniques, are also being proposed for independent actuation using local measurements [49]. Although machine-learning techniques allow for the adaptive configuration of controllers for maintaining feasibility in infrastructure operation, optimality or efficiency cannot be guaranteed due to the lack of coordination among other nodes in the system and empirically derived control parameters.

Summary of independent coordination

Independent coordination involves no communication, and decisions are made using the local measurements of system states. This myopic technique is simple and not subject to unexpected delays or vulnerabilities in the cyberchannel. However, achieving guarantees on efficiency and optimality while accounting for all-important state variables, such as reactive/real power-flow and bus-voltage magnitude/frequencies with no access to the global system state, is not practical, as summarized in Table 5. Thus, independent coordination is highly suited for such applications as primary control, where response time is critical, and not for optimal operations.

Integrated hierarchical decision making

The power grid is a highly coupled and complex system composed of many diverse and fluctuating power components. We have presented a detailed exposition on the tractable modeling of the electrical characteristics/limits of the existing grid infrastructure, associated system stakeholders (e.g., TNs, DNs, microgrids, power consumers), and decision-making paradigms (i.e. centralized, distributed, decentralized, and independent coordination). Tractable modeling of the underlying physical attributes of the system is imperative to efficiently integrate highly unpredictable power components. Various

Table 5. A summary of independent coordination techniques.

Method	Optimality	Feasibility	Convergence
Droop control	No guarantee	Feasible	Not relevant
Primal-dual dynamics	Guaranteed	No guarantee for voltage	Asymptotic
Machine learning	No guarantee	Feasible	Not relevant

Table 6. A summary of hierarchical framework.

Tier	Structure	Topology	Horizon	Complexity
1	TN, microgrid	Decentralized	~10 min	$O(n)$
2	DN, IPP	Distributed	~10 s	$O(k)$
2	Bulk generation, buildings	Centralized	~10 s	$O(m^p)$
3	Governor, inverter	Independent	~10 ms	$O(c)$

grid stakeholders in the power grid enable the natural decomposition of the power system into manageable counterparts. Decision-making topologies are associated with advantages and tradeoffs that render these suitable for a wide variety of grid applications. Thus, these must be cohesively combined into a grid-coordination framework that enables the seamless plug-and-play integration of power components into the system and adaptive response by actuating nodes to keep the system efficient and the grid resilient. For this, a hierarchical approach is needed.

The main principles for designing a hierarchical grid coordination framework are called *abstraction* and *decoupling*. The optimal power-flow problem $\mathcal{P}_c$ can be constructed for the entire power grid where the cost of operation of individual components is minimized while adhering to complex nonconvex grid constraints. If every single component of the power grid (e.g., power lines and consumers/suppliers) is included in this problem, then the problem will involve millions of variables related to each other in a highly nonlinear manner. Since directly solving this problem is practically impossible, the coordination problem must be divided into tractable subproblems that are more manageable and contained. This is established by leveraging the natural hierarchy of the power grid. The TN is composed of buses that represent DNs, bulk synchronous generators, and/or IPPs. A DN is composed of buses that represent a set of residential, industrial, or commercial consumers. Bulk synchronous generators consist of active controllers that adjust mechanical input to vary real/reactive-power output as necessary. IPPs can be large farms consisting of many solar panels or wind turbines with inverters that can be controlled to supply real/reactive power based on available generation capacities. Thus, the coordination problem can be narrowed down from a high-level context to a specific case.

Moreover, the coordination horizon is unique for various coordination applications. For instance, in the planning stage, the coordination period will be lengthier (in the scale of minutes) than primary control processes that entail fast-acting responses (in the scale of milliseconds). Also, the coordination structure will be different for each stakeholder due to the inherent management attributes of these components. At the TN or microgrid level, due to deregulation and the participation of independent suppliers/consumers, decentralized coordination is appropriate since no central authority is necessary. In the DN, distributed coordination is appropriate due to the presence of the EPU with access to aggregate system measurements. Within individual consumers (e.g., buildings and so on) and bulk-generation systems, centralized coordination can be used to manage local appliances or mechanical systems, such as governors. To adapt to transience in the system, independent coordination can be leveraged to maintain operations around optimal setpoints computed in higher layers. This is summarized in Table 6, where k, p, and c are constants, and n and m reflect the number of entities in the system.

In the hierarchical system defined in Figure 14, it is clear that the abstraction and coordination interval increases when ascending the framework. Thus, in the higher tiers, planning

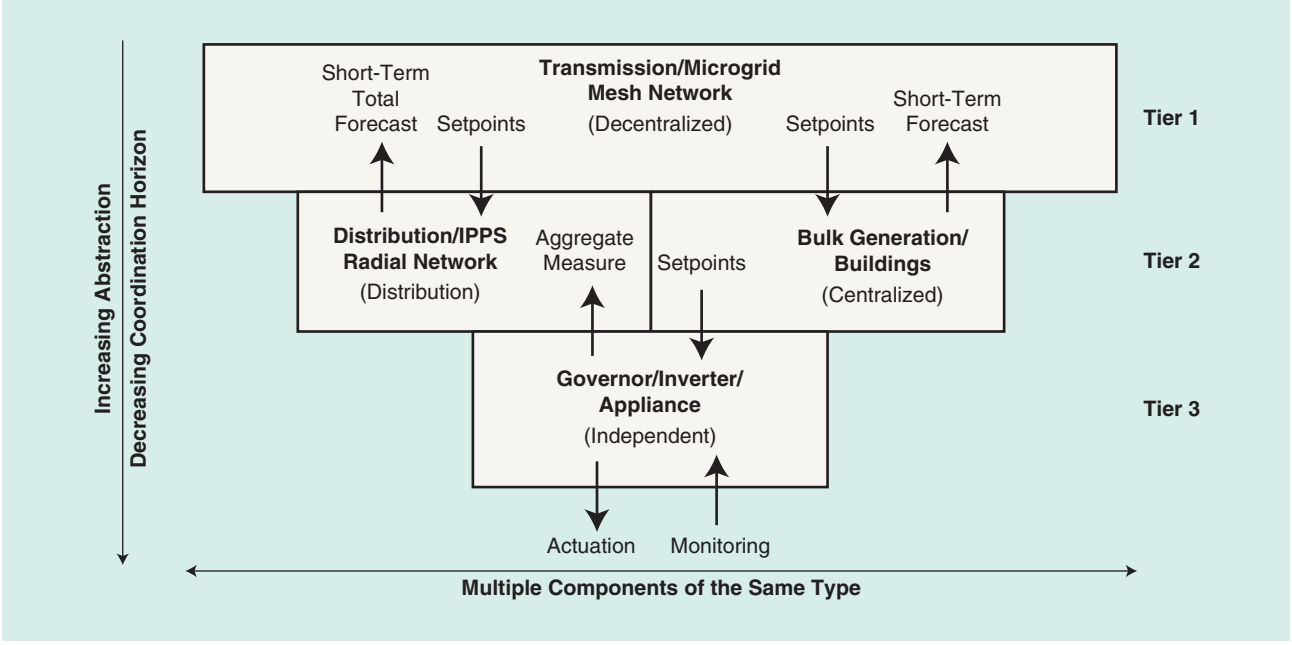

FIGURE 14. The detailed hierarchical framework.

is prevalent, and, in the lower tiers, actuation is the primary focus. In the subsequent tiers, optimal setpoints computed for the coordination problem formulated for the underlying system are refined based on the decoupling and decomposition in effect. The coordination interval allocated accommodates the complexity of the coordination problem at hand. For instance, at the TN level, decentralized coordination has a complexity of $O(n)$. If each signaling iteration takes place every 10 ms to account for the communication latency in the order of milliseconds, then 1,000 iterations can take place within the 10-min coordination horizon. As illustrated in Figure 12, convergence in a 2,736-bus system occurs within 100 iterations. Thus, the allocated coordination horizon is more than sufficient for computing optimal setpoints for individual TN buses every 10 min. This optimal setpoint represents the real-power injection into the TN bus by either DNs, IPPs, and/or bulk synchronous systems that reside in the subsequent tier. Then these systems coordinate local entities, such as power consumers and DGs, to maintain this optimal setpoint. These entities, such as power consumers, compute the optimal demand setpoint over 10-s intervals. Individual elements residing within the consumer premises locally actuate to maintain this refined setpoint via independent coordination. As the longest coordination interval is 10 min, fluctuation in the demand and generation can be accurately accommodated via short-term forecasts.

Thus, the proposed hierarchical framework allows for the fluid coordination of individual power entities by way of abstraction and decomposition. This flexibility and cohesiveness in coordination can effectively accommodate the continuously changing landscape of the modern power grid. Although hierarchical management is not a unique concept (e.g., [50] and [51]), our work is a novel departure due to the granularity of optimization, scalability, and the integration of various communication topologies based on the underlying physical constraints.

The hierarchical coordination framework presented in this article focuses on the power infrastructure. The main elements considered in the design of this framework are the structure of the network being coordinated, the tractable relaxation of the system model, and the decomposition of the coordination problem into simpler subproblems. The process used in this article to identify common trends and underlying distinguishing patterns for coordination purposes can be readily applied in any interdependent processes or networked systems, such as manufacturing processes, communication networks (e.g., software-defined systems), and water-power flow systems. Thus, hierarchical coordination is transferrable to a wide variety of applications.

Conclusions and future directions

The rapidly evolving nature of the modern power grid necessitates leveraging signal processing for all-encompassing coordination among diverse actuating power components. Given the complex, connected, and collaborative nature of the cyberphysical smart grid, a unified signal processing framework is essential to determine and devise efficient grid dynamics and operations while incorporating physical constraints.

The first step in the construction of this grid-coordination framework by way of signal processing is to model system interactions tractably. Relaxations and approximations must retain the discerning characteristics of physical relations among power components while enabling scalability so that these can be used to construct signals that summarize general trends in the system with respect to the physical grid. Realistic formulations available in the state of the art of these relations in four specific constituents of the power grid (TNs, DNs, microgrids, and power consumers) are presented. Then, these are leveraged in four different decision-making topologies that govern the construction and exchange of monitoring/control signals that facilitate adaptive actuation by individual power entities. The signals convey generalized information about the external environment. This information is used to perform adaptive actuation while heeding local infrastructure limits. Finally, these decision-making topologies are organized into a hierarchical framework for specific power-system components that capitalize on abstraction and decomposition derived using a tractable optimal power-flow formulation for signal processing that enables all-encompassing grid coordination. This unified framework enables the seamless plug-and-play integration of heterogeneous and intermittent power-system components at all levels of the smart grid while accounting for the underlying physical attributes of the system.

As future work, we intend to extend this hierarchical signal-processing framework to detect and mitigate cyberphysical attacks, ensure small-signal/transient stability, and address power-quality issues. Moreover, it is also of interest to identify how the signal processing framework proposed in this article for the energy sector can be extended to other domains.

Authors

Pirathayini Srikantha (psrikan@uwo.ca) received her B.A.Sc. degree in systems design engineering in 2009 and her M.A.Sc. degree in electrical and computer engineering in 2013, both from the University of Waterloo, Canada. She received her Ph.D. degree in electrical and computer engineering from the University of Toronto, Canada, in 2017. She is an assistant professor in the Department of Electrical and Computer Engineering at Western University, Canada. She is a certified Professional Engineer in Ontario, Canada. Her research interests include large-scale optimization and distributed control in the power grid. Her research efforts have been recognized in premier conference venues. She is a Member of the IEEE.

Deepa Kundur (dkundur@ece.utoronto.ca) received her B.A.Sc., M.A.Sc., and Ph.D. degrees all in electrical and computer engineering in 1993, 1995, and 1999, respectively, from the University of Toronto, Canada, where she is a professor of electrical and computer engineering and serves as the chair of the Division of Engineering Science. Her research interests span the fields of signal processing, cyberphysical systems, and complex dynamical networks. She is an author of more than 200 journal and conference papers and has served as the

general chair for a variety of technical meetings, including several GlobalSIP symposia. She is a Fellow of the IEEE and the Canadian Academy of Engineering. She also serves on the Advisory Board of *IEEE Spectrum*.

References

[1] H. Farhangi, "The path of the smart grid," *IEEE Power Energy Mag.*, vol. 8, no. 1, pp. 18–28, 2010.

[2] H. Gharavi, A. Scaglione, M. Dohler, and X. Guan, "Technical challenges of the smart grid: From a signal processing perspective," *IEEE Signal Process. Mag.*, vol. 29, no. 5, pp. 12–13, 2012.

[3] J. D. Glover, T. Overbye, and M. Sarma, *Power System Analysis and Design*. Boston: Cengage Learning, 2016.

[4] T. Cutsem and C. Vournas, *Voltage Stability of Electric Power Systems*. New York: Springer, 2008.

[5] G. Kortuem, F. Kawsar, V. Sundramoorthy, and D. Fitton, "Smart objects as building blocks for the Internet of Things," *IEEE Internet Comput.*, vol. 14, no. 1, pp. 44–51, 2010.

[6] A. Finamore, V. Galdi, V. Calderaro, A. Piccolo, G. Conio, and S. Grasso, "Artificial neural network application in wind forecasting: An one-hour-ahead wind speed prediction," in *Proc. IET Int. Conf. Renewable Power Generation*, 2016, pp. 1–6.

[7] P. Srikantha and D. Kundur, "Hierarchical signal processing for tractable power flow management in electric grid networks," *IEEE Trans. Signal Informat. Process. Netw.*, 2018. doi: 10.1109/TSIPN.2018.2858750.

[8] S. Boyd and L. Vandenberghe, *Convex Optimization*. Cambridge, UK: Cambridge Univ. Press, 2004.

[9] J. A. Taylor, *Convex Optimization of Power Systems*. Cambridge, UK: Cambridge Univ. Press, 2015.

[10] K. G. Murty and S. N. Kabadi, "Some NP-complete problems in quadratic and nonlinear programming," *Math. Programming*, vol. 39, no. 2, pp. 117–129, 1987.

[11] S. Diamond, R. Takapoui, and S. Boyd, "A general system for heuristic solution of convex problems over non-convex sets," *Optimization Methods Software*, vol. 33, no. 1, pp. 165–193, 2018.

[12] D. Lee, P. Srikantha, and D. Kundur, "Secure operating region simplification in dynamic security assessment," in *Proc. IEEE Smart Grid Communication Conf.*, 2015, pp. 79–84.

[13] A. Von Meier, *Electric Power Systems: A Conceptual Introduction*. Hoboken, NJ: Wiley, 2006.

[14] Ontario's Power Authority. (2017). Ontario's long-term energy plan. Ministry of Energy, Northern Development and Mines, Toronto, ON, Canada. [Online]. Available: https://www.ontario.ca/page/ontarios-long-term-energy-plan

[15] R. D. Zimmerman, C. E. Murillo-Sanchez, and R. J. Thomas, "MATPOWER: Steady-state operations, planning and analysis tools for power systems research and education," *IEEE Trans. Power Syst.*, vol. 26, no. 1, pp. 12–19, 2011.

[16] Z. Yang, H. Zhong, Q. Xia, and C. Kang, "A novel network model for optimal power flow with reactive power and network losses," *Electric Power Syst. Res.*, vol. 144, no. 1, pp. 63–71, 2017.

[17] Z. Yang, H. Zhong, Q. Xia, A. Bose, and C. Kang, "Optimal power flow based on successive linear approximation of power flow equations," *IET Generation, Transmission Distribution*, vol. 10, no. 14, pp. 3654–3662, 2016.

[18] C. Coffrin and P. V. Hentenryck, "A linear-programming approximation of AC power flows," *INFORMS J. Computing*, vol. 26, no. 4, pp. 718–734, 2014.

[19] J. Pillai, P. Thogersen, J. Moller, and B. Bak-Jensen, "Integration of electric vehicles in low voltage Danish distribution grids," in *Proc. IEEE Power and Energy Society General Meeting*, 2012, pp. 1–8.

[20] C. W. Gellings, M. Samotyj, and B. Howe, "The future's smart delivery system," *IEEE Power Energy Mag.*, vol. 2, no. 5, pp. 40–48, 2004.

[21] P. Srikantha, C. Rosenberg, and S. Keshav, "An analysis of peak demand reductions due to elasticity of domestic appliances," in *Proc. ACM/IEEE Int. Conf. Future Energy Systems*, 2012, pp. 1–11.

[22] S. H. Low, "Convex relaxation of optimal power flow part I: Formulations and equivalence," *IEEE Trans. Control Netw. Syst.*, vol. 1, no. 1, pp. 15–27, 2014.

[23] L. Gan, U. Topcu, and S. Low, "Exact convex relaxation of optimal power flow in radial networks," *IEEE Trans. Autom. Control*, vol. 60, no. 1, pp. 72–87, 2015.

[24] D. E. Olivares, A. Mehrizi-Sani, A. H. Etemadi, C. A. Canizares, R. Iravani, M. Kazerani, A. H. Hajimiragha, O. Gomis-Bellmunt, M. Saeedifard, R. Palma-Behnke, G. A. Jimenez-Estevez, and N. D. Hatziargyriou, "Trends in microgrid control," *IEEE Trans. Smart Grid*, vol. 5, no. 4, pp. 1905–1919, 2014.

[25] A. Etemadi, E. J. Davison, and R. Iravani, "A decentralized robust control strategy for multi-DER microgrids–Part I: Fundamental concepts," *IEEE Trans. Power Del.*, vol. 27, no. 4, pp. 1843–1853, 2012.

[26] P. Palensky and D. Dietrich, "Demand side management: Demand response, intelligent energy systems, and smart loads," *IEEE Trans. Ind. Informat.*, vol. 7, no. 3, pp. 381–388, 2011.

[27] P. Srikantha and D. Kundur, "A novel evolutionary game theoretic approach to real-time distributed demand response," in *Proc. IEEE Power & Engineering Society General Meeting*, 2015, pp. 1–5.

[28] M. Pham-Hung, P. Srikantha and D. Kundur, "A secure cloud architecture for data generated in the energy sector," in *Proc. EAI Int. Conf. Smart Grids*, 2015, pp. 374–383.

[29] H. Quan, D. Srinivasan, and A. Khosravi, "Short-term load and wind power forecasting using neural network-based prediction intervals," *IEEE Trans. Neural Netw. Learn. Syst.*, vol. 25, no. 2, pp. 303–315, 2014.

[30] D. Kundur, X. Feng, S. Liu, T. Zourntos, and K. L. Butler-Purry, "Towards a framework for cyber attack impact analysis of the electric smart grid," in *Proc. IEEE Smart Grid Communication Conf.*, 2010, pp. 1–6.

[31] P. Srikantha and D. Kundur, "Distributed optimal of dispatch in sustainable generation systems via dual decomposition," *IEEE Trans. Smart Grid*, vol. 6, no. 5, pp. 2501–2509, 2015.

[32] S. Boyd, L. Xiao, and A. Mutapcic, "Subgradient methods," Lecture notes for EE393o, Stanford Univ., Palo Alto, CA. 2003.

[33] D. Bertsekas, A. Nedic, and A. E. Ozdaglar, *Convex Analysis and Optimization*. Nashua, NH: Athena Scientific, 2003.

[34] P. Srikantha and D. Kundur, "Distributed demand curtailment via water-filling," in *Proc. IEEE Smart Grid Communication Conf.*, 2015, pp. 1–5.

[35] W. H. Sandholm, *Population Games and Evolutionary Dynamics*. Cambridge, MA: MIT Press, 2009.

[36] P. Srikantha and D. Kundur, "Resilient distributed real-time demand response via population games," *IEEE Trans. Smart Grid*, vol. 8, no. 6, pp. 2532–2543, 2017.

[37] P. Srikantha and D. Kundur, "A game theoretic approach to real-time robust distributed generation dispatch," *IEEE Trans. Ind. Informat.*, vol. 13, no. 3, pp. 1006–1016, 2016.

[38] P. Srikantha and D. Kundur, "Real-time integration of intermittent generation with voltage rise considerations," *IEEE Trans. Sustain. Energy*, vol. 8, no. 3, pp. 938–952, 2016.

[39] Q. Peng and S.H. Low, "Distributed algorithm for optimal power flow on an unbalanced radial network," in *Proc. IEEE Conf. Decision and Control*, 2015, pp. 1–6.

[40] C. Chen, J. Wang, and S. Kishore, "A distributed direct load control approach for large-scale residential demand response," *IEEE Trans. Power Syst.*, vol. 29, no. 5, pp. 2219–2228, 2014.

[41] B. Golub and M. O. Jackson, "Network structure and speed of learning," *Ann. Economics Statist.*, vol. 107, no. 108, pp. 33–48, 2012.

[42] S. Boyd, N. Parikh, E. Chu, B. Peleato, and J. Eckstein, "Distributed optimization and statistical learning via the alternating direction method of multipliers," *Foundations Trends Mach. Learning*, vol. 3, no. 1, pp. 1–122, 2010.

[43] D. Monderer and L. S. Shapley, "Potential games," *Games Economic Behaviour*, vol. 14, no. 1, pp. 124–143, 1996.

[44] T. Ui, "Discrete concavity for potential games," *Int. Game Theory Rev.*, vol. 10, no. 1, pp. 1–8, 2008.

[45] A. M. Eldurssi and R. M. O'Connell, "A fast non-dominated sorting guided genetic algorithm for multi-objective power distribution system reconfiguration problem," *IEEE Trans. Power Syst.*, vol. 30, no. 2, pp. 593–601, 2015.

[46] V. Gungor, D. Sahin, T. Kocak, S. Ergut, C. Buccella, C. Cecati, G. Hancke, and D. Kundur, "Smart grid technologies: Communication technologies and standards," *IEEE Trans. Ind. Informat.*, vol. 7, no. 4, pp. 529–539, 2011.

[47] C. Zhao, U. Topcu, N. Li, and S. Low, "Design and stability of load-side primary frequency control in power systems," *IEEE Trans. Autom. Control*, vol. 59, no. 5, pp. 1177–1189, 2014.

[48] H. Kakigano, Y. Miura, and T. Ise, "Distribution voltage control for DC microgrids using fuzzy control and gain-scheduling technique," *IEEE Trans. Power Electron.*, vol. 28, no. 5, pp. 2246–2258, 2013.

[49] R. R. Negenborn, A. G. Beccuti, T. Demiray, S. Leirens, G. Damm, B. De Schutter, and M. Morari, "Supervisory hybrid model predictive control for voltage stability of power networks," in *Proc. American Control Conf.*, 2007, pp. 5444–5449.

[50] R. J. Sanchez-Garcia, M. Fennelly, S. Norris, N. Wright, G. Niblo, J. Brodzki, and J. W. Bialek, "Hierarchical spectral clustering of power grids," *IEEE Trans. Power Syst.*, vol. 29, no. 5, pp. 2229–2237, 2014.

[51] P. Tian, X. Xiao, K. Wang, and R. Ding, "A hierarchical energy management system based on hierarchical optimization for microgrid community economic operation," *IEEE Trans. Smart Grid*, vol. 7, no. 5, pp. 2230–2241, 2016.

SP